European Journal of Medicinal Chemistry 107 (2016) 275–287

Contents lists available at ScienceDirect

European Journal of Medicinal Chemistry

journal homepage: http://www.elsevier.com/locate/ejmech

Research paper

3-(Dipropylamino)-5-hydroxybenzofuro[2,3-*f*]quinazolin-1(2*H*)-one (DPA-HBFQ-1) plays an inhibitory role on breast cancer cell growth and progression

Pietro Rizza [a, 1], Michele Pellegrino [a, 1], Anna Caruso [a, 1], Domenico Iacopetta [a, 1], Maria Stefania Sinicropi [a, **], Sylvain Rault [b, ***], Jean Charles Lancelot [b], Hussein El-Kashef [c], Aurelien Lesnard [b], Christophe Rochais [b], Patrick Dallemagne [b], Carmela Saturnino [d], Francesca Giordano [a], Stefania Catalano [a], Sebastiano Andò [a, *]

[a] Department of Pharmacy, Health and Nutritional Sciences, University of Calabria, 87036, Arcavacata di Rende, Italy
[b] Université de Caen Basse-Normandie, Centre d'Etudes et de Recherche sur le Médicament de Normandie UPRES EA 4258, FR CNRS 3038 INC3M, Bd Becquerel, 14032 Caen Cedex, France
[c] Department of Chemistry, Faculty of Science, Assiut University, 71516 Assiut, Egypt
[d] Department of Pharmacy, University of Salerno, Via Giovanni Paolo II 132, 84084 Fisciano, Salerno, Italy

ARTICLE INFO

Article history:
Received 2 July 2015
Received in revised form
5 October 2015
Accepted 3 November 2015
Available online 10 November 2015

Keywords:
3-(Alkyl(dialkyl)amino)-benzofuro[2,3-*f*]quinazolin-1(2*H*)-one analogs
3-(dipropylamino)-5-hydroxybenzofuro[2,3-*f*]quinazolin-1(2*H*)-one
Dibenzofuran derivatives
One-pot reaction
Apoptosis

ABSTRACT

A series of unknown 3-(alkyl(dialkyl)amino)benzofuro[2,3-*f*]quinazolin-1(2*H*)-ones **4**–**17** has been synthesized as new ellipticine analogs, in which the carbazole moiety and the pyridine ring were replaced by a dibenzofuran residue and a pyrimidine ring, respectively. The synthesis of these benzofuroquinazolinones **4**–**17** was performed in a simple one-pot reaction using 3-aminodibenzofuran or its 2-methoxy derivative, as starting materials. From 3-(dipropylamino)-5-methoxybenzofuro[2,3-*f*] quinazolin-1(2*H*)-one (**13**), we prepared 3-(dipropylamino)-5-hydroxybenzofuro[2,3-*f*]quinazolin-1(2*H*)-one (**18**), referred to as **DPA-HBFQ-1**. The cytotoxic activities of all the synthesized compounds, tested in different human breast cancer cell lines, revealed that **DPA-HBFQ-1** was the most active compound. In particular, the latter was able to inhibit anchorage-dependent and -independent cell growth and to induce apoptosis in estrogen receptor alpha (ERα)-positive and -negative breast cancer cells. It did not affect proliferation and apoptotic responses in MCF-10A normal breast epithelial cells. The observed effects have been ascribed to an enhanced $p21^{Cip1/WAF1}$ expression in a p53-dependent manner of tumor suppressor and to a selective inhibition of human topoisomerase II. In addition, **DPA-HBFQ-1** exerted growth inhibitory effects also in other cancer cell lines, even though with a lower cytotoxic activity. Our results indicate **DPA-HBFQ-1** as a good candidate to be useful as cancer therapeutic agent, particularly for breast cancer.

1. Introduction

Breast cancer (BC) is the second most frequent malignancy and the most common cancer among women in the industrialized countries [1,2]. It represents a significant cause of death in spite of the advances in the anticancer therapies and the improvement of disease-free and overall survival of patients with BC. The first-line of treatment consists of both radiotherapy and chemotherapy either alone or in combination with surgery [3]. Most of the chemotherapeutic drugs remain the treatment of choice especially for metastasis, but they are often associated with severe side effects. Thus, there is always a need to develop new, more powerful and selective drugs with low side effects, which can represent a valid alternative to the current pharmacological approaches [4–6]. A variety of chemotherapeutics deleteriously damage DNA inducing different outcomes, such as replication and transcription blockage, mutagenesis and eventually cell death [7,8]. The possibility of

* Corresponding author.
** Corresponding author.
*** Corresponding author.
E-mail addresses: s.sinicropi@unical.it (M.S. Sinicropi), sylvain.rault@unicaen.fr (S. Rault), sebastiano.ando@unical.it (S. Andò).
[1] These authors contributed equally to the manuscript.

http://dx.doi.org/10.1016/j.ejmech.2015.11.004
0223-5234/

Abbreviations

DPA-HBFQ-1	3-(dipropylamino)-5-hydroxybenzofuro[2,3-*f*] quinazolin-1(2*H*)-one
BC	Breast Cancer
DMF	DiMethylFormamide
rt	room temperature
h	hours
eq.	equivalent
MCF-7	Michigan Cancer Foundation-7
MCF-10A	Michigan Cancer Foundation-10A
MTT	Methylthiazol Tetrazolium Assay
MDA-MB-231	M.D. Anderson Metastatic Breast -231
HeLa	Henrietta Lacks
p53	protein 53
$p21^{Cip1/WAF1}$	protein 21
mRNA	Messenger Ribonucleic Acid
SD	Standard Deviation
RT-PCR	Real Time Polymerase Chain Reaction
cDNA	complementary DeoxyRibonucleic Acid
GAPDH	Glyceraldehyde 3-Phosphate Dehydrogenase
bp	base pair
siRNA	silencing Ribonucleic Acid
WT	Wild Type
Δp53	Deleted p53 sites
pGL3	plasmid GL3
ADP	Adenosine Diphosphate
PARP	Poly Adenosindiphosphate-Ribose Polymerase
MCF-7 TR1	Michigan Cancer Foundation Tamoxifen-resistant 1
MS (EI)	Electrospray Ionization Mass Spectrometry
m/z	mass/charge
LC-MS	Liquid Cromatography Mass Spectrometry
^{1}H NMR	proton Nuclear Magnetic Resonance
^{13}C NMR	Carbon Nuclear Magnetic Resonance
δ	chemical shift
$CDCl_3$	deuterated chloroform
DMSO-d_6	deuterated dimethyl sulfoxide
ppm	part per millions
s	singlet
d	doublet
t	triplet
q	quartet
m	multiplet
J	coupling constant
Hz	hertz
TLC	thin layer cromatography
mmol	millimoles
IR	Infrared
Mp	Melting point
Et_2O	diethyl ether
DMEM	Dulbecco's Modified Eagle Medium
CMV	Cytomegalovirus
DNase I	Deoxyribonuclease I
NP-40	NonidetP-40
ECL	Enhanced Chemiluminescence
SYBR green	Synergy Brands Inc. green
ATCC	American Type Culture Collection
FBS	Fetal Bovine Serum
DMEM-F12	Dulbecco's Modified Eagle Medium F12
MEM	Minimal Essential Medium
luc	luciferase
SDS-PAGE	Sodium Dodecyl Sulfate PolyAcrilamide Gel Electrophoresis
PBS	Phosphate Buffer Saline
RNase	Ribonulcease
RNAi	Ribonuclease Acid interference
IC_{50}	Inhibitory Concentration 50
ANOVA	Analysis of Variance.

resistance onset to chemotherapy is strictly dependent on DNA repair efficiency in tumor cells [9–11]. Amongst a plethora of anticancer DNA-targeted drugs, ellipticine (5,11-dimethyl-6*H*-pyrido[4,3-*b*]carbazole) [12,13] (Fig. 1), an alkaloid derived from the leaves of the evergreen tree *Ochrosia elliptica* [14] with a tetracyclic planar structure [15], has been found to be a potent antineoplastic agent exhibiting multiple mechanisms of action [16–19].

The anticancer action of ellipticine and its analogs [20] is based mainly on DNA damage, *via* intercalation into DNA, inhibition of topoisomerases, and formation of covalent DNA adducts mediated by CYPs and peroxidases [14,21–30].

Ellipticine induces apoptosis in malignant cells with activation of both the mitochondrial and death receptor pathways of caspase [31]. Several studies have reported that ellipticine also changes the tumor suppressor p53 conformation from mutant to wild type, restores the sequence-specific DNA binding and transactivation of p53-driven luciferase reporter, and activates mutant p53 to induce p53 target genes, p21 and Mdm2 in mouse xenograft tumor tissues [31–33].

However, the therapeutic applications and beneficial effects of ellipticine remain limited because the onset of some side effects [17]. Under this point of view, the search for new ellipticine derivatives that exhibit a higher antitumoral activity but less adverse effects is always appreciated. Therefore, numerous libraries of carbazole derivatives and carbazole isosteres (such as pyrimidocarbazoles, pyrrolopyrazinocarbazoles, benzofuropyrroloquinoxalines, pyridazinocarbazoles, benzofurophtalazines, benzothienoquinolines, benzofuroquinolines, benzothieno-, benzofuropyrrolopyrazines-, pyrido[3,2-b] carbazoles, and many others) have been described [34].

More recently, a large number of ellipticine derivatives have been synthesized and tested for antitumor activity in preclinical models [35–39].

In this study we present the synthesis of new planar fused tetracyclic heterocycles, as ellipticine homologs structurally correlated to 2-dialkylamino-5,11-dimethyl-6*H*-pyrimido-[5,4-*b*]carbazol-4(3*H*)-ones [12], namely 3-(alkyl(dialkyl)amino)benzofuro [2,3-*f*] quinazolin-1(2*H*)-ones **4**–**17** (Fig. 2) and of 3-(dipropylamino)-5-

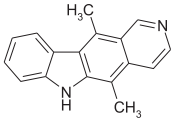

Fig. 1. Structure of ellipticine.

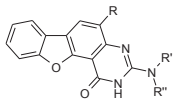

Fig. 2. Benzofuroquinazolinone derivatives.

hydroxybenzofuro[2,3-*f*]quinazolin-1(2*H*)-one (**18**) referred to as **DPA-HBFQ-1**.

Furthermore, we have demonstrated that some compounds of this series exhibited a moderate antiproliferative activity, whereas the derivative **DPA-HBFQ-1** exerted higher and interesting biological activities, inducing growth inhibition and apoptosis of breast cancer cells, and Tamoxifen-resistant breast cancer cells. This occurs through the specific inhibition of topoisomerase II, the up-regulation of p53 and the enhanced $p21^{Cip1/WAF1}$ gene expression. Moreover, **DPA-HBFQ-1** showed a good cytotoxic activity on rat Leydig tumor cells R2C, human Ishikawa endometrial cancer cells, cervical cancer HeLa and human hepatoma HepG2 cells. These outcomes appear very promising for the development of new approaches to cancer treatment, especially in case of drug resistance occurrence.

2. Results and discussion

2.1. Chemistry

3-Aminodibenzofurans **1a-b**, were used as starting materials in the synthesis of a series of new 3-(alkyl(dialkyl)amino)benzofuro[2,3-*f*]quinazolin-1(2*H*)-ones **4**–**17** *via* a one-pot three-component reaction (Scheme 1) [29,34,40]. Compound **1a** was prepared, however, according to a reported method [41]. The amino derivatives **1a-b** were reacted with ethoxycarbonylisothiocyanate, to give the thiourea intermediates **2**, followed by the addition of the appropriate alkylamine or dialkylamine and $HgCl_2$ to give the ethoxycarbonylguanidine intermediates **3**. The latter intermediates were subjected to thermal cyclization at 160 °C in the same reaction medium followed by filtration of the HgS by-product to give the 3-(alkyl(dialkyl)amino)benzofuro[2,3-*f*]quinazolin-1(2*H*)-ones **4**–**17**, respectively. This sequential one-pot three-component synthesis proved to be rapid, simple and efficient.

It is worthy to note that at the end of the reaction, all the mercury salt used was recovered as a black precipitate of HgS, and the absence of mercury in the final samples has been verified by mass spectrometry.

Finally, considering that several ellipticine analogues, active as antitumor agents (*e.g.* Elliptinium [42,43]), possess a hydroxy group as substituent on the tetracyclic nucleus, the methoxy derivative **13** underwent demethylation, upon heating in anhydrous pyridine hydrochloride under reflux, to give the 3-(dipropylamino)-5-hydroxybenzofuro[2,3-*f*] quinazolin-1(2*H*)-one **(18, DPA-HBFQ-1)** with moderate yield (30%) (Scheme 2).

In addition to the common IR bands and NMR signals of both compounds **13** and **18**, the IR spectrum of compound **18** is characterized by the presence of a stretching vibration band at 3390 cm^{-1} corresponding to the O–H at position 5. Its ^1H NMR spectrum showed this O–H group as broad signal at 8.23 ppm. Moreover, the ^1H NMR spectrum of **13** is characterized by a third CH_3 signal at 3.95 ppm corresponding to the OCH_3 group at position 5.

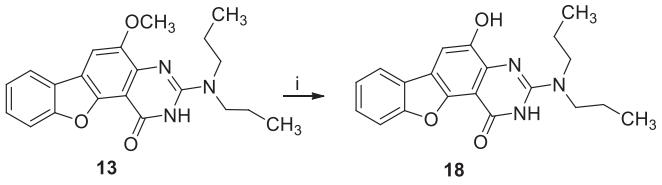

Scheme 2. Reagents: (i) anhydrous pyridine hydrochloride (5 eq.), reflux, 2 h.

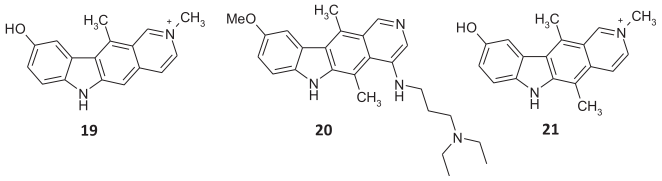

Fig. 3. Structure of 2-Methyl-9-hydroxyellipticinium (**19**), Retelliptine (**20**) and Elliptinium (**21**).

2.2. Biology

2.2.1. Inhibitory effect of DPA-HBFQ-1 on breast cancer cell growth

The idea behind the synthesis of our library of ellipticine analogs was inspired from the interesting biological activities of ellipticine. Since its isolation, approximately five decades ago, a large number of ellipticine derivatives have been synthesized and evaluated for their antitumor activity in preclinical models and, as well, some of them reached phase I in clinical trials [43,44], in particular 2-methyl-9-hydroxyellipticinium (**19**) and Retelliptine (**20**), while Elliptinium (**21**) was tested in phase II clinical trials (Fig. 3) [43].

These compounds showed moderate antitumor activity in patients with metastatic breast cancer [42,45] along with toxic effects [21].

In this context, we have synthesized novel compounds **4**–**18,** as carbazoles bioisosters, to be evaluated for their effects on breast cancer cells growth. The human $ER\alpha^+$ (MCF-7) and $ER\alpha^-$ (MDA-MB-231) breast cancer cell lines, and breast non-tumorigenic epithelial cells (MCF-10A) were used for this study. The synthesized 3-alkyl(dialkyl)aminobenzofuro[2,3-*f*] quinazolin-1(2*H*)-ones **4**–**17** and the 3-dipropylamino-5-hydroxybenzofuro[2,3-*f*]quinazolin-1(2*H*)-one **(18, DPA-HBFQ-1),** which structures have been reported in Table 1 and Scheme 2, respectively, were evaluated on cell proliferation using MTT assay [30,46,47] (Figure S1).

Some of these compounds, particularly **6, 7** and **8**, showed moderate antigrowth properties in MCF-7 cells, equal to 10%, 25% and 15% respect to vehicle-treated cells, highlighting the importance of the dialkyl substituents on nitrogen in position 3. Next, we introduced a methoxy group in position 5 and amongst these derivatives only the three compounds **12, 13** and **14** appeared to be active, exhibiting the 15%, 37% and 25% of cell proliferation inhibition, respectively (Figure S1).

Similar results have been obtained in MDA-MB-231 cell lines,

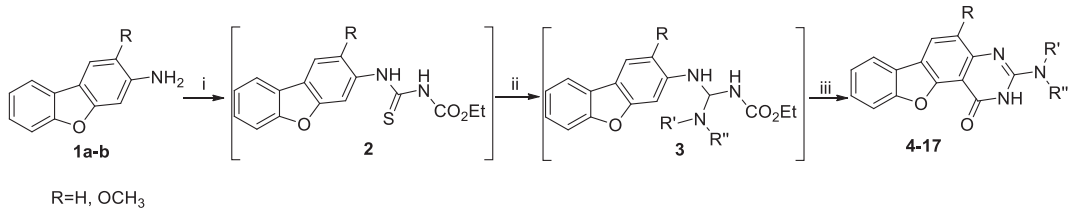

Scheme 1. Reagents: (i) EtOCONCS (1 eq.), DMF, 4 h, rt; (ii) alkylamines or dialkylamines (3 eq.), $HgCl_2$ (1 eq.), 10 min, 0 °C, then 18 h, rt; (iii) 2 h, 160 °C.

Table 1
Library of 3-(alkyl(dialkyl)amino)benzofuro[2,3-*f*]quinazolin-1(2*H*)-ones **4**–**17**.

Compounds	R	R′	R″
4	H	H	$(CH_2)_2CH_3$
5	H	H	$(CH_2)_3CH_3$
6	H	CH_2CH_3	CH_2CH_3
7	H	$(CH_2)_2CH_3$	$(CH_2)_2CH_3$
8	H	$(CH_2)_3CH_3$	$(CH_2)_3CH_3$
9	H	Pyrrolidin-1-yl	_
10	H	Morpholin-1-yl	_
11	H	Piperidin-1-yl	_
12	OCH_3	CH_2CH_3	CH_2CH_3
13	OCH_3	$(CH_2)_2CH_3$	$(CH_2)_2CH_3$
14	OCH_3	$(CH_2)_3CH_3$	$(CH_2)_3CH_3$
15	OCH_3	Pyrrolidin-1-yl	_
16	OCH_3	Morpholin-1-yl	_
17	OCH_3	Piperidin-1-yl	_

whereas we did not notice any effect on human normal breast derived cell line, MCF-10A, vitality (data not shown).

Based on these outcomes, we decided to maintain the dipropyl group on the nitrogen in position 3 (compound **13**) and to replace the present 5-methoxy group with a hydroxyl group, obtaining the **DPA-HBFQ-1**.

The latter structural modification improved the antiproliferative activity; indeed the treatment with **DPA-HBFQ-1** at 1 μM for 5 days has been able to reduce cell viability in MCF-7 (58%) and MDA-MB-231 (60%). Furthermore, **DPA-HBFQ-1** did not elicit any significant inhibitory activity in MCF-10A cells (Figure S2A), under the same conditions. The IC_{50} values were 33.00 ± 0.30 μM, 0.66 ± 0.04 μM and 0.65 ± 0.03 μM in MCF-10A, MCF-7 and MDA-MB-231 cells, respectively (Figure S2B) for **DPA-HBFQ-1,** and 1.20 ± 0.20 μM, 1.25 ± 0.30 μM and 1.82 ± 0.15 μM for ellipticine, respectively, used as reference molecule. The antiproliferative activity mediated by this molecule has been evaluated using anchorage-independent soft agar growth assay. Consistently with MTT assays, **DPA-HBFQ-1** treatment significantly reduced colony formation in both breast cancer cells (Figure S2C).

2.2.2. *DPA-HBFQ-1 increased p21$^{Cip1/WAF1}$ proteins in breast cancer cells in p53-dependent manner*

Numerous studies reported that the cytotoxic activity induced by ellipticine is mediated by the tumor-suppressor protein p53 [48,49], which functions generally as a transcription factor able to induce growth arrest or apoptosis of damaged or malignant cells. Approximately 55% of human tumors have genetically identifiable loss of p53 function [50], and it has been shown that ellipticine is responsible of p53 nuclear stabilization by restoring its sequence-specific DNA binding and transcription function [28,31,34]. Through this mechanism, ellipticine induces cell cycle progression arrest [26,28] or, in turn, may indirectly inhibit ubiquitination preventing the nuclear export of p53. To determine whether the cell growth inhibition activity of **DPA-HBFQ-1** was mediated by changes in cell cycle regulatory proteins, we examined the effects of treatment on p53 and p21$^{Cip1/WAF1}$ expression (Fig. 4A), in human normal breast derived cell line, MCF-10A, and in human breast cancer cell lines, MCF-7 and MDA-MB-231. Cells were treated with **DPA-HBFQ-1** at 0.1 μM and 1 μM concentrations for 48h and whole cell lysates were analyzed using immunoblotting assay. As shown in Fig. 4A, we did not observe any significant variation in the levels of p53 and p21$^{Cip1//WAF1}$ in MCF-10A cells. In contrast, the treatment with **DPA-HBFQ-1** resulted in an increase of p53 and p21$^{Cip1/WAF1}$ protein expression in MCF-7 and MDA-MB-231 cells, in a dose dependent manner. In the same experimental condition, we observed a significant up-regulation of p21$^{Cip1/WAF1}$ mRNA levels in both breast cancer cells, but no change of p53 mRNA levels (Fig. 4B), suggesting how the increase of p53 upon **DPA-HBFQ-1** exposure, is essentially due to an enhanced p53 stability.

2.2.3. *DPA-HBFQ-1 transactivated p21$^{Cip1/WAF1}$ gene promoter via p53 binding site*

Since p21$^{Cip1/WAF1}$ is one of the best-characterized *bona fide* p53 target genes, we focused our attention on p21 promoter gene. Several evidences reported that the human p21$^{Cip1/WAF1}$ promoter has two p53 binding sites (or response elements, REs) that conform to the p53 consensus binding sequence (Fig. 5A): the more distal (5′) site at −2283 bp that binds p53 relatively strongly and the more proximal (3′) site at −1391 bp that binds p53 more weakly [42,43,48,51–53]. The above-mentioned evidences prompted us to investigate whether **DPA-HBFQ-1** could transactivate the p21$^{Cip1/WAF1}$ promoter gene. Thus, MCF-7 cells were transiently transfected with a luciferase reporter construct containing the upstream region of the p21$^{Cip1/WAF1}$ gene spanning from −2320 to +300 bp, and treated with **DPA-HBFQ-1** (0.1 μM and 1 μM) for 24 h. We found a significant activation of p21$^{Cip1/WAF1}$ after treatment with **DPA-HBFQ-1**. Conversely, we observed that in breast cancer cells transiently transfected with a construct containing p21$^{Cip1/WAF1}$ promoter lacking p53 consensus sequences, **DPA-HBFQ-1** was no longer able to induce p21$^{Cip1/WAF1}$ promoter activity (Fig. 5B). Similar results were obtained in MDA-MB-231 cells (data not shown).

To demonstrate that the down-regulatory effects induced by **DPA-HBFQ-1**exposure on p21$^{Cip1/WAF1}$ promoter were exclusively mediated by p53, we transfected MCF-7 cells with p21$^{Cip1/WAF1}$ full length construct in the presence of p53 siRNA. As expected, in the latter conditions, the activation of p21$^{Cip1/WAF1}$ promoter was no longer noticeable (Fig. 5C). This well correlates with the dramatically reduction of the up-regulatory effects on p21$^{Cip1/WAF1}$ protein content, induced by **DPA-HBFQ-1**, in the same experimental condition (Fig. 5D).

Taken together, our findings demonstrated the crucial role of p53 in **DPA-HBFQ-1-**induced up-regulation of p21$^{Cip1/WAF1}$. These functional studies evidenced, then, the ability of **DPA-HBFQ-1** to up-regulates p21$^{Cip1/WAF1}$ promoter gene and that this transactivation was dependent on p53, since p21$^{Cip1/WAF1}$ promoter construct deleted of p53 response elements was no longer able to be activated from **DPA-HBFQ-1** exposure. Indeed, the crucial role of p53 in mediating the inhibitory activity of **DPA-HBFQ-1** in p21 $^{Cip1/WAF1}$ activation and expression was definitively demonstrated in breast cancer cells through the p53 silencing.

2.2.4. *DPA-HBFQ-1 induced apoptosis in breast cancer cells*

Given that p53 and p21$^{Cip1/WAF1}$ induce apoptotic cascade, acting as tumor suppressor genes, we investigated whether **DPA-HBFQ-1** treatment could induce cell death by apoptosis in our model system. First, we evaluated the proteolysis of poly (ADP-ribose) polymerase (PARP), a known substrate of effector caspases, by immunoblotting analysis (Figure S3A). We found an increase in the protein levels of the proteolytic form of PARP (116 kDa) in MCF-7 cells under **DPA-HBFQ-1** treatment, while PARP-cleavage levels were unchanged in MCF-10A cells. Subsequently, we determined whether **DPA-HBFQ-1** treatment may induce changes in the internucleosomal fragmentation profile of genomic DNA, a diagnostic hallmark of cells undergoing apoptosis (Figure S3B). Marked DNA fragmentation in MCF-7 cells was evidenced after 48 h exposure with **DPA-HBFQ-1**. Again, no DNA fragmentation was observed in the normal breast cell line. Similar results were obtained in MDA-MB-231 cells (data not shown).

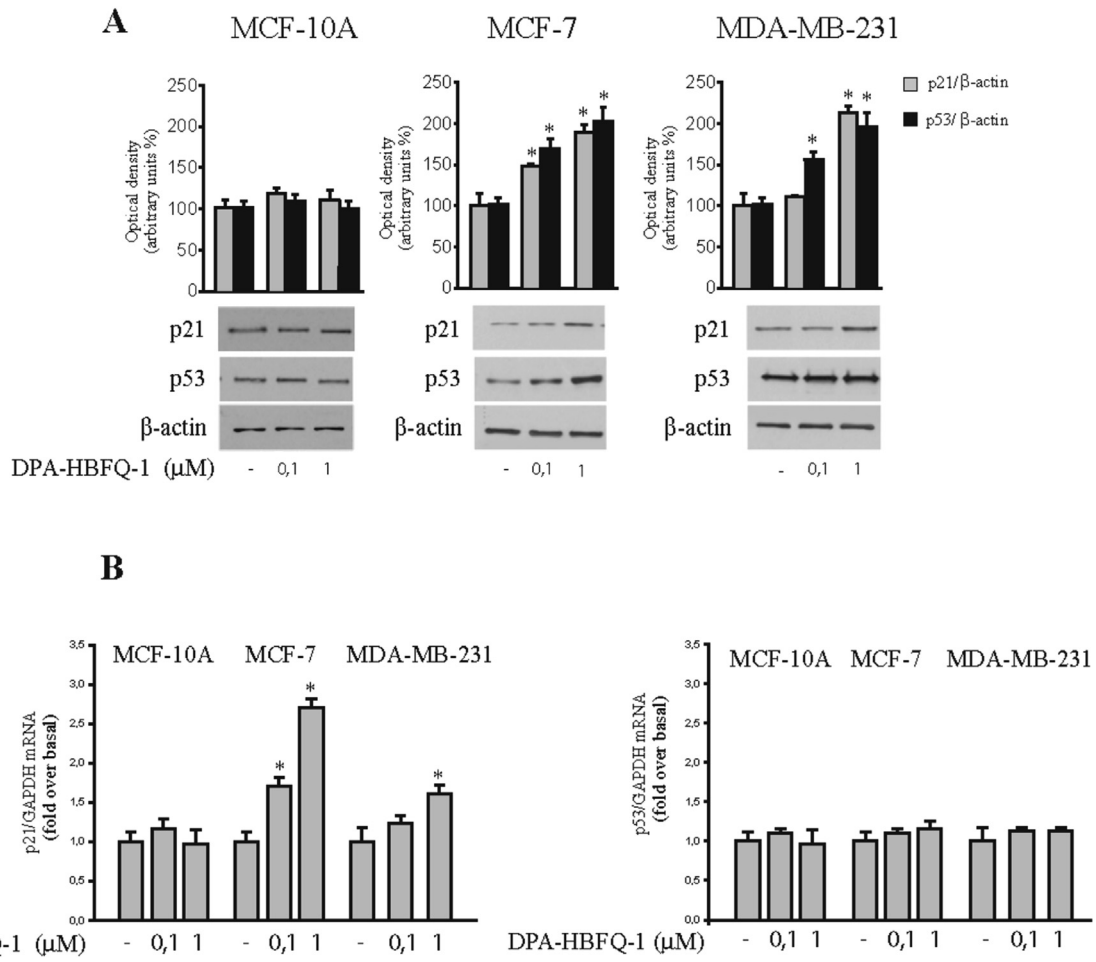

Fig. 4. Expression of p53 and $p21^{Cip1/WAF1}$ levels after **DPA-HBFQ-1** treatment in breast cancer cells. A: Bottom panel, immunoblots of p53, and $p21^{WAF1/Cip1}$ from extracts of MCF-10A, MCF-7 and MDA MB-231 cells treated with vehicle (−) or **DPA-HBFQ-1** at 0.1 μM and 1 μM of concentrations for 48 h β-Actin was used as control for equal loading. Upper panel, the histograms represent the mean ± SD of three separate experiments in which band intensities were evaluated in terms of optical density arbitrary units and expressed as percentage of control which was assumed to be 100%. B: MCF-10A, MCF-7 and MDA MB 231 cells were treated with vehicle (−) or **DPA-HBFQ-1** 0.1 μM and 1 μM for 12 h. Total RNA was isolated from cells and reverse transcribed. cDNA was subjected to real time RT-PCR using primers specific for p53, $p21^{WAF1/Cip1}$ and GAPDH. Each sample was normalized to its GAPDH mRNA content. Data represent the mean ± S.D. of values from three separate RNA samples expressed as percentage of control assumed to be 100%. *P < 0.05 compared to vehicle-treated cells.

2.2.5. DPA-HBFQ-1 inhibited MCF-7 Tamoxifen-resistant breast cancer cells growth

The onset of acquired tamoxifen resistance represents a crucial and high-frequency therapeutic problem which, over the years, became a very attractive field of study for many researchers. Several molecular mechanisms were proposed to be responsible of tamoxifen resistance occurrence and tumors relapse, so that the discovery of new pharmacological tools or targets is still challenging. Under this point of view, we addressed our attention to the capability of **DPA-HBFQ-1** to affect growth of Tamoxifen-resistant malignant breast cells (MCF-7 TR-1) by using MTT assay and anchorage-independent soft agar growth assay (Fig. 6A and B). After 3 and 5 days of treatment, we observed that **DPA-HBFQ-1** reduced the cell vitality; in addition the compound inhibited colony formation of MCF-7 TR-1 after 14 days of treatment. These results appear to be correlated with clonogenic assay experiments, demonstrating that **DPA-HBFQ-1** is able to reduce cell colony formation in Tamoxifen-resistant breast cancer cells (Fig. 6C). The calculated IC_{50} values for **DPA-HBFQ-1** and ellipticine were of 1.0 ± 0.2 μM and 1.75 ± 0.3 μM, respectively.

Moreover, upon **DPA-HBFQ-1** treatment (0.1 μM and 1 μM) we also observed an up-regulation of p53 and $p21^{Cip1/WAF1}$ expression (Fig. 6D), a marked DNA fragmentation and an increase in the levels of the proteolytic form of PARP (Fig. 6E and F). These findings are in agreement with the experiments previously discussed and performed in MCF-7 and MDA-MB-231 cancer cell lines and highlight, again, the potential development of **DPA-HBFQ-1** as alternative and/or adjuvant compound, also in hormonal-resistant breast cancer therapy.

2.2.6. DPA-HBFQ-1 inhibitory activity on human Topoisomerase I and II

Many literature data reported that ellipticine is able to interfere with DNA-metabolizing enzymes, such as topoisomerases [54,55]. With the aim to test if the most active compound **DPA-HBFQ-1,** structurally correlated to ellipticine, could act as topoisomerases poison, we performed inhibition assays using human topoisomerase I and II. No inhibition activity on human topoisomerase I was observed (Fig. 7, panel A) upon **DPA-HBFQ-1** exposure at the two doses used in this assay (10 and 50 μM), so that the enzyme is able to produce relaxed topoisomers (lanes 6 and 7). The same compound was able to inhibit topoisomerase II activity in a dose dependent manner (Fig. 7, panel B, lanes 7 and 8), resulting in a fail of intact kDNA migration on agarose gel (because its big size). In the

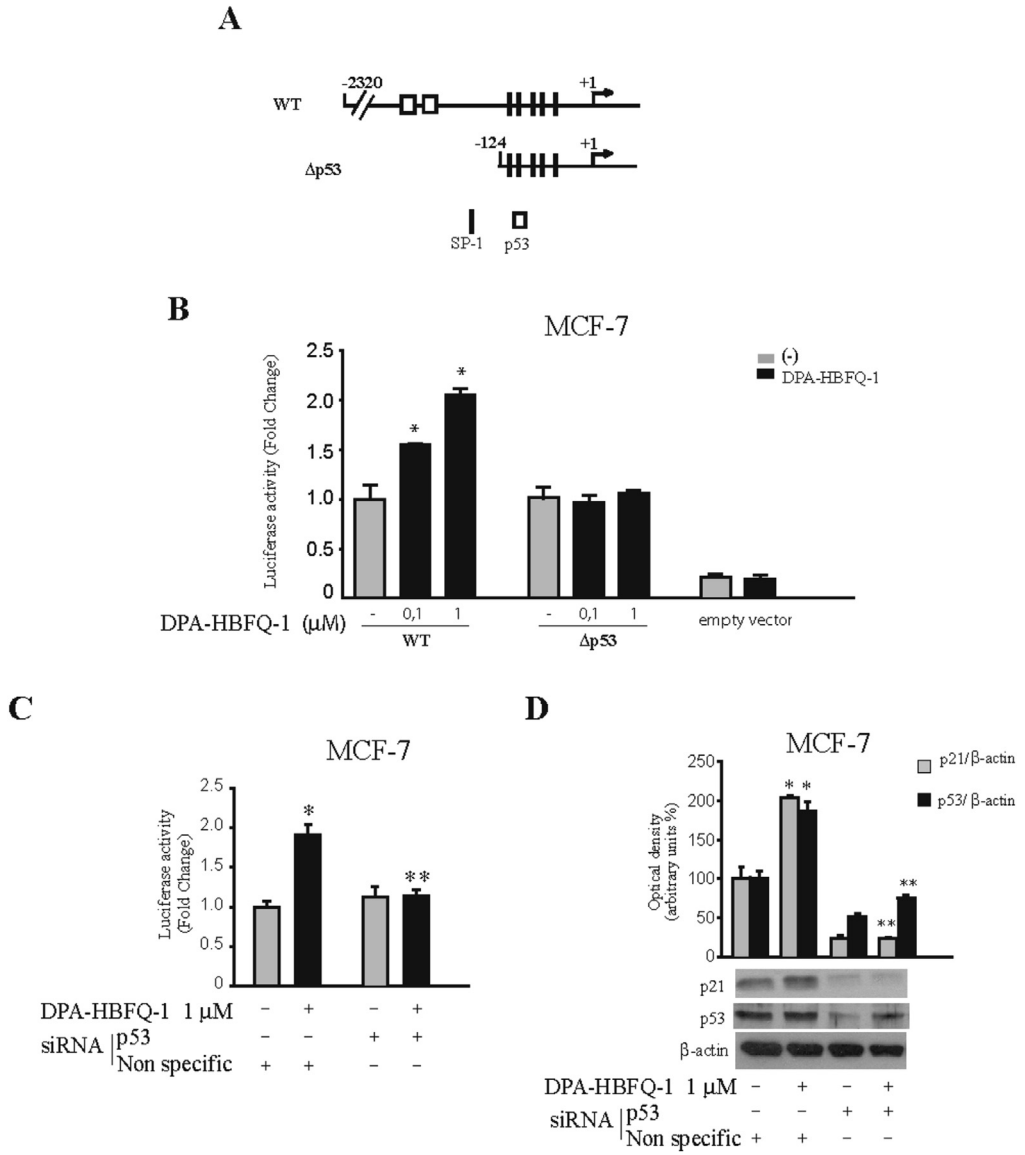

Fig. 5. DPA-HBFQ-1 induces the transcriptional activity of p21$^{Cip1/WAF1}$ promoter gene. A: Schematic map of the p21$^{Cip1/WAF1}$ promoter plasmids used in this study. B: MCF-7 cells were transiently transfected with the wild-type p21 $^{Cip1/WAF1}$ promoter luciferase (WT) and with deleted construct (Δp53) and then treated with vehicle (−) or **DPA-HBFQ-1** 1 μM. Luciferase activities were normalized to the Renilla Luciferase as internal transfection control and data where reported as fold change. The values represent the means ± SD of three different experiments each performed in triplicate. Empty vector: basal activity measured in cells transfected with empty vector basal vector. *P < 0.01 compared to vehicle-treated cells. C: MCF-7 cells were transiently transfected with the wild-type p21 $^{Cip1/WAF1}$ promoter luciferase and then treated with vehicle (−) or **DPA-HBFQ-1** 1 μM in the presence of a non-specific or a p53 siRNA. Luciferase activities were normalized to the Renilla Luciferase as internal transfection control and data where reported as fold change. The values represent the means ± SD of three different experiments each performed in triplicate. pGL3: basal activity measured in cells transfected with empty vector. *$P < 0.01$ compared to vehicle-treated cells, **P < 0.05 compared to **DPA-HBFQ-1** treated cells. D: Western Blot analysis for p21$^{Cip1/WAF1}$ and p53 expression in cells treated with vehicle (−) or **DPA-HBFQ-1** for 48 h in the presence of a non-specific or a p53 siRNA. β-actin was used as loading control. The histograms represent the mean ± SD of three independent experiments in which band intensities were evaluated in terms of optical density arbitrary units and expressed as the percentage of the control assumed to be 100%. *$P < 0.01$ compared to vehicle-treated cells, **P < 0.05 compared to **DPA-HBFQ-1** treated cells.

control experiment (vehicle) the enzyme binds kDNA and releases intact monomeric rings visible at the bottom of gel as two DNA bands, which represent the nicked open circular minicircles and fully closed circular rings (decatenation products, lane 4). A linear DNA product (lane 3) has also been loaded on gel, in order to exclude any production of linear DNA under these conditions. In these assays, we used ellipticine as reference molecule, which has been already reported to be a strong and non-specific topoisomerase I and II inhibitor and, as well, a DNA intercalating agent [54,55]. Ellipticine clearly blocked human topoisomerases I and II (Fig. 7, panel A, lanes 4 and 5, panel B, lanes 5 and 6) and behaved as a typical intercalator, binding DNA and inducing an electrophoretic mobility shift both in pHOT1 (panel A, lanes 4 and 5, single band consistent with supercoiled DNA) and in kDNA decatenated products (panel B, lane 5). Thus, **DPA-HBFQ-1** showed a behavior different to that of ellipticine, because it did not inhibit topoisomerase I activity and was not been able to intercalate DNA, being, instead, a selective inhibitor of human topoisomerase II in dose dependent manner. These results well correlate and strengthen the previously discussed effects on p53and p21$^{Cip1//WAF1}$ up-regulation elicited by **DPA-HBFQ-1**, responsible of the antitumor activity via apoptosis induction.

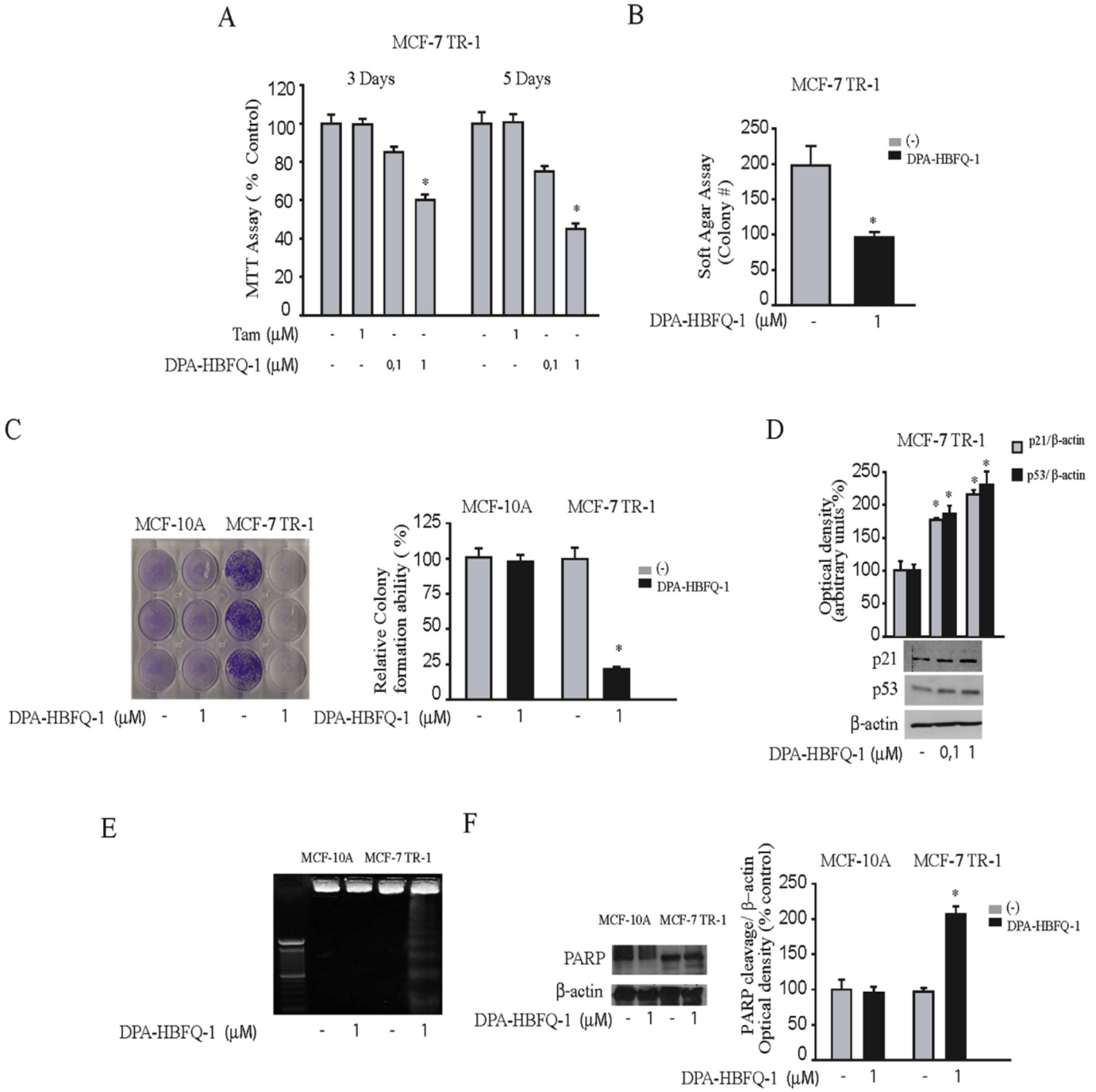

Fig. 6. Activity of **DPA-HBFQ-1** on Tamoxifen-resistant breast cancer cells. A: MTT assays in MCF-10A and MCF-7 TR-1 cells treated with vehicle (−), or **DPA-HBFQ-1** at 0.1 μM and 1 μM for 3 and 5 days. Cell proliferation is expressed as % of control (vehicle-treated cells). The values represent the means ± SD of three different experiments, each performed with triplicate samples. *P < 0.05 compared to vehicle-treated cells. B: MCF-7 TR-1 cells were plated in soft agar and then treated with vehicle (−) or with **DPA-HBFQ-1** (0.1 μM and 1 μM). Cells were allowed to grow for 14 days and the number of colonies >50 μm were quantified and the results were graphed. Data are the mean colony number ±SD of three plates of three independent experiments. *P < 0.05 compared to vehicle-treated cells. C: Left panel, effects of **DPA-HBFQ-1** on MCF-10A and MCF-7 TR-1 colony formation as measured by clonogenic assay. Cells were treated with **DPA-HBFQ-1** 1 μM then cultured for 14 days. Survival colonies were stained with Crystal Violet. Right panel, the histograms represent the means ± SD of three separate experiments in which band intensities were evaluated in terms of relative colony formation ability arbitrary and expressed as percentage of control which was assumed to be 100%. *P < 0.05 compared to vehicle-treated cells. D: Left panel, immunoblots of p53, and $p21^{Cip1/WAF1}$ from extracts of MCF-10A and MCF-7 TR-1 cells treated with vehicle (−) or **DPA-HBFQ-1** at 1 μM for 48 h β-Actin was used as control for equal loading. Right panel, the histograms represent the mean ± SD of three separate experiments in which band intensities were evaluated in terms of optical density arbitrary units and expressed as percentage of control which was assumed to be 100%. *P < 0.05 compared to vehicle-treated cells. E: DNA laddering performed in MCF-10A and MCF-7 TR-1 cells treated with vehicle (−) or **DPA-HBFQ-1** (1 μM) for 48 h. One of three similar experiments is presented. F: Left panel, immunoblots of PARP protein from extracts of MCF-10A and MCF-7 TR-1 cells treated with vehicle (−) or **DPA-HBFQ-1** at 1 μM for 48 h β-Actin was used as control for equal loading and transfer. Right panel, the histograms represent the means ± SD of three separate experiments in which band intensities were evaluated in terms of optical density arbitrary units and expressed as percentage of control which was assumed to be 100%. *P < 0.05 compared to vehicle-treated cells.

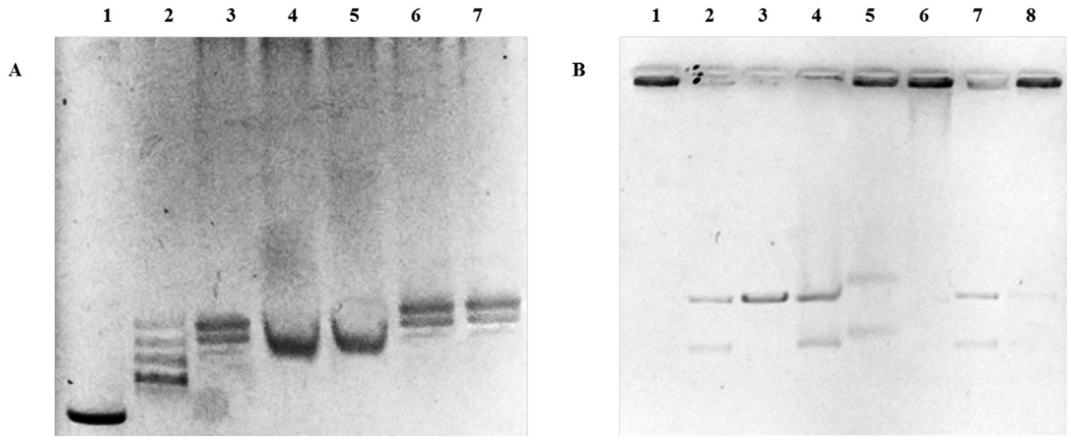

Fig. 7. Human topoisomerase I and II assays. A: relaxation assay. Supercoiled DNA was incubated without or with human topoisomerase I in the absence or presence of the test compounds at the indicated doses: Lane 1, super coiled DNA, lane 2, relaxed DNA marker, lane 3, vehicle (DMSO), lane 4 and 5, ellipticine 10 and 50 μM respectively, lane 6 and 7, **DPA-HBFQ-1** 10 and 50 μM respectively. B: decatenation assay. kDNA was incubated without or with human topoisomerase II in the absence or presence of the test compounds at the indicated doses: Lane 1, kDNA, lane 2, decatenated DNA marker, lane 3, linear kDNA, lane 4, vehicle (DMSO), lane 5 and 6, ellipticine 10 and 50 μM respectively, lane 7 and 8, **DPA-HBFQ-1** 10 and 50 μM respectively.

2.2.7. Cytotoxic activity of DPA-HBFQ-1 on different cancer cell lines

The cytotoxic activity of **DPA-HBFQ-1** was evaluated, as well, on others tumor cell lines, *i.e.* rat Leydig tumor cells R2C, human Ishikawa endometrial cancer cells, cervical cancer HeLa and human hepatoma HepG2 cells. The IC_{50} values were determined and showed in Table 2, using ellipticine as reference molecule. The results indicated that **DPA-HBFQ-1** exerted a good anti-proliferative activity not only in breast cancer cells but also in the above mentioned cancer cell lines, most probably due to the above discussed biological activities that could be confirmed in further studies, even though in a less extent. These latter outcomes make this compound of particular pharmaceutical interest, broadening its potential therapeutic applications.

3. Conclusions

In summary a new library of fourteen carbazole bioisosters, namely 3-alkyl(dialkyl)aminobenzofuro[2,3-*f*]quinazolin-1(2*H*)-ones **4**–**17**, was synthesized in a sequential one-pot three-component reaction, starting from 3-aminodibenzofurans, and assayed on breast cancer cells showing a moderate antiproliferative activity. Out of this library, the derivative **DPA-HBFQ-1**, prepared starting from **13**, showed an effective growth inhibition in ERα^{+}, ERα^{-} and tamoxifen-resistant breast cancer cell lines, without affecting the growth of normal epithelial breast cells. These effects are mediated by the ability of compound **DPA-HBFQ-1** to up-regulate the cell cycle regulators p53 and p21$^{Cip1//WAF1}$ and to selectively inhibit the human topoisomerase II. Moreover, its cytotoxic activity was assessed also on different cancer cell lines with promising outcomes. Our results might be seminal for future studies regarding **DPA-HBFQ-1** as potential pharmacological tool to be implemented in the novel strategies for breast cancer treatment, also in the occurrence of resistance to hormonal therapies.

Table 2
Effects of **DPA-HBFQ-1** on growth inhibition of different cancer cell lines. IC_{50} values were reported in μM and represents the mean ± SD of three separate experiments.

	R2C	Ishikawa	HeLa	HepG2
DPA-HBFQ-1	1.20 ± 0.1	0.98 ± 0.2	0.70 ± 0.1	0.89 ± 0.3
ellipticine	2.0 ± 0.2	1.50 ± 0.3	1.00 ± 0.2	2.90 ± 0.3

4. Experimental section

4.1. Synthesis and characterization

Commercial reagents were purchased from Aldrich, Acros Organics and Alfa Aesar and used without additional purification. Melting points were determined on a Kofler melting point apparatus. Elemental analyses were performed at the "Institut de Recherche en Chimie Organique Fine" (Rouen). The IR spectra were recorded on a Perkin Elmer BX FT-IR using KBr wafer technique. Mass spectra were taken on a JEOL JMS GCMate spectrometer at ionising potential of 70 eV (EI) or were performed using a spectrometer LC-MS Waters alliance 2695 (ESI+). ^{1}H NMR (400 MHz for ^{1}H, 100 MHz for the ^{13}C) 1H and ^{13}C NMR chemical shifts (δ) were reported in parts per million (ppm) and were referenced to the solvent peak; $CDCl_3$ (7.26 ppm for ^{1}H and 76.90 ppm for ^{13}C) and DMSO-d_6 (2.50 ppm for ^{1}H and 39.70 ppm for ^{13}C). Multiplicities are represented by s (singlet), d (doublet), t (triplet), q (quartet) and m (multiplet). Coupling constants (J) are reported in Hertz (Hz). Thin layer chromatography (TLC) was performed on silica gel 60F-264 (Merck). 3-Aminodibenzofuran **(1a)** was prepared as described in the literature [41] and the 3-amino-2-methoxy-dibenzofuran **(1b)** was purchased from Sigma–Aldrich.

4.1.1. General procedure for the preparation of 3-(alkyl(dialkyl) amino)benzofuro[2,3-f] quinazolin-1(2H)-ones (4–17)

To a solution of the 3-aminodibenzofuran **(1a)** or 3-amino-2-methoxy-dibenzofuran **(1b)** (2.67 mmol) in DMF (40 mL), ethoxycarbonylisothiocyanate (2.67 mmol) was added and the reaction mixture was stirred at room temperature (RT) for 4 h. The reaction mixture was then cooled to 0 °C, the alkyl(dialkyl)amine (6.67 mmol) was added, followed by the addition of $HgCl_2$ (2.67 mmol) and the resulting mixture was stirred at RT overnight. The reaction mixture was then heated under reflux at 160 °C for 2 h, cooled, filtered through a celite pad and concentrated in vacuum. The solid obtained was crystallized from acetonitrile.

4.1.1.1. 3-(Propylamino)benzofuro[2,3-f]quinazolin-1(2H)-one (***4***). Brown powder (25% yield). Mp > 260 °C. IR (KBr) (cm^{-1}): 3344 (ν NH), 2959 (ν CH arom.), 2874 (ν CH aliph.), 1674 (ν C=O), 1636 (ν C=N), 1518 (ν C=C), 1475 (ν C=C), 1340, 1186, 740, 634. ^{1}H NMR (DMSO-d_6): δ 0.94–1.07 (t, 3H, CH_3), 1.50–1.70 (m, 4H, $CH_2CH_2CH_3$),

6.55 (br, 1H, N*H*), 7.35–7.55 (m, 3H, *Ar*), 7.75 (d, 1H, *J* = 8.10 Hz, *Ar*), 8.10 (d, 1H, *J* = 7.20 Hz, *Ar*), 8.30 (d, 1H, *J* = 8.76 Hz, *Ar*), 11.10 (br, 1H, N*H*). ^{13}C NMR (DMSO-d_6): 161. 00 (C=O), 156. 57 (C10a), 155.76 (C3), 153.56 (C11a), 148.90 (C4a), 146.26 (C6b), 130.02 (C6), 126.21 (C9), 123.39 (C8), 123.33 (C7), 119.97 (C5), 119.72 (C10), 111.98 (C11b), 100.31 (C6a), 48.89 (CH_2), 21.72 (CH_2), 11.58. (CH_3). MS (EI) *m/z* (%): 293 ($M^{+\cdot}$, 100), 278 (39) ($M^{+\cdot} - CH_3$), 264 (100) ($M^{+\cdot} - CH_2CH_3$), 235 (77) ($M^{+\cdot} - CH_2CH_2CH_3$). Anal. Calcd for $C_{17}H_{15}N_3O_2$: C, 69.61; H, 5.15; N, 14.33. Found: C, 69.64; H, 5.11; N, 14.36.

*4.1.1.2. 3-(Butylamino)benzofuro[2,3-f]quinazolin-1(2H)-one (**5**).* White powder (25% yield). Mp > 260 °C. IR (KBr) (cm^{-1}): 3260 (ν NH), 3046 (ν CH arom.), 2958 (ν CH aliph.), 2864 (ν CH aliph.), 1681 (ν C=O), 1634 (ν C=N), 1457 (ν C=C), 1348, 1186, 712. ^{1}H NMR (DMSO-d_6): δ 0.90–0.95 (t, 3H, CH_3), 1.23–1.38 (m, 2H, CH_2CH_3), 1.55–1.60 (m, 2H, $CH_2CH_2CH_2CH_3$), 3.48–3.52 (m, 2H, $NCH_2(CH_2)_2CH_3$), 6.40 (br, 1H, N*H*), 7.30–7.60 (m, 3H, *Ar*), 7.65–7.90 (m, 1H, *Ar*), 8.15 (d, 1H, *J* = 7.80 Hz, *Ar*), 8.40 (d, 1H, *J* = 7.80 Hz, *Ar*), 11.10 (br, 1H, N*H*). ^{13}C NMR (DMSO-d_6): 159.87 (C=O), 156. 43 (C10a), 155.46 (C3), 153.45 (C11a), 150.27 (C4a), 147.21 (C6b), 129.04 (C6), 126.23 (C9), 123.37 (C8), 123.11(C7), 119.83 (C5), 119.77 (C10), 111.27 (C11b), 101.23 (C6a), 45.98 (CH_2), 30.38 (CH_2), 18.96 (CH_2), 13.04 (CH_3). MS (ESI^+): 308 (M^+ +1). Anal. Calcd for $C_{18}H_{17}N_3O_2$: C, 70.34; H, 5.58; N, 13.67. Found: C, 70.31; H, 5.60; N, 13.70.

*4.1.1.3. 3-(Diethylamino)benzofuro[2,3-f]quinazolin-1(2H)-one (**6**).* Orange powder (50% yield). Mp > 260 °C. IR (KBr) (cm^{-1}): 3334 (ν NH), 3119 (CH arom.), 2977 (ν CH aliph.), 2932 (ν CH aliph.), 1668 (ν C=O), 1596 (ν C=C), 1457 (ν C=C), 1304, 1187, 1021, 819, 739. ^{1}H NMR (DMSO-d$_6$): δ 1.10–1.15 (t, 6H, NCH_2CH_3), 3.57–3.61 (q, 4H, NCH_2CH_3), 7.25 (br, 1H, N*H*), 7.26–7.50 (m, 3H, *Ar*), 7.76 (d, 1H, *J* = 8.04 Hz, *Ar*), 8.06 (d, 1H, *J* = 7.60 Hz, *Ar*), 8.25 (d, 1H, *J* = 8.52 Hz, *Ar*). ^{13}C NMR (DMSO-d_6): 160.31 (C=O), 155.04 (C10a), 154.89 (C3), 152.83 (C11a), 149.99 (C4a), 144.30 (C6b), 126.03 (C6), 125.92 (C9), 123.40 (C8), 123.32 (C7), 120.43 (C5),119.92 (C10), 111.66 (C11b), 102.34 (C6a), 41.53 ($2CH_2$), 13.26 ($2CH_3$). MS (EI) *m/z* (%): 307 ($M^{+\cdot}$, 100), 278 (100) ($M^{+\cdot} - C_2H_5$). Anal. Calcd for $C_{18}H_{17}N_3O_2$: C, 70.34; H, 5.58; N, 13.67. Found: C, 70.37; H, 5.55; N, 13.69.

*4.1.1.4. 3-(Dipropylamino)benzofuro[2,3-f]quinazolin-1(2H)-one (**7**).* Yellow powder (30% yield). Mp = 246 °C. IR (KBr) (cm^{-1}): 3346 (ν NH), 3135 (ν CH arom.), 2963 (ν CH aliph.), 1662 (ν C=O), 1583 (ν C=C), 1456 (ν C=C), 1186, 825, 745, 519. ^{1}H NMR (DMSO-d_6): δ 0.82–0.92 (t, 6H, CH_3), 1.50–1.70 (m, 4H, CH_2CH_3), 3.45–3.55 (t, 4H, $NCH_2CH_2CH_3$), 7.22 (d, 1H, *J* = 8.70 Hz, *Ar*), 7.30–7.50 (m, 2H, *Ar*), 7.75 (d, 1H, *J* = 8.01 Hz, *Ar*), 8.08 (d, 1H, *J* = 7.60 Hz, *Ar*), 8.25 (d, 1H, *J* = 8.58 Hz, *Ar*), 11.25 (br, 1H, N*H*). ^{13}C NMR (DMSO-d_6): 161.98 (C=O), 157.32 (C10a), 155.61 (C3), 153.34 (C11a), 147.80 (C4a), 146.20 (C6b), 129.02 (C6), 125.86 (C9), 123.37 (C8), 123.29 (C7), 119.87 (C5), 119.72 (C10), 111.63 (C11b), 100.01 (C6a), 48.78 ($2CH_2$), 20.72 ($2CH_2$), 10.98 ($2CH_3$). MS (EI) *m/z* (%): 335 ($M^{+\cdot}$, 100), 306 (75) ($M^{+\cdot} - CH_2CH_3$), 292 (61) ($M^{+\cdot} - CH_2CH_2CH_3$). Anal. Calcd for $C_{20}H_{21}N_3O_2$: C, 71.62; H, 6.31; N, 12.53. Found: C, 71.59; H, 6.34; N, 12.55.

*4.1.1.5. 3-(Dibutylamino)benzofuro[2,3-f]quinazolin-1(2H)-one (**8**).* White powder (48% yield). Mp = 192 °C. IR (KBr) (cm^{-1}): 3129 (ν NH), 3051 (CH arom.), 2958 (CH aliph.), 2869 (CH aliph.), 1660 (ν C=O), 1592 (ν C=C), 1457 (ν C=C), 1176, 1020, 743. ^{1}H NMR (DMSO-d_6): δ 0.89–0.94 (t, 6H, $(CH_2)_3CH_3$), 1.28–1.40 (m, 4H, $(CH_2)_2CH_2CH_3$), 1.50–1.60 (m, 4H, $CH_2CH_2CH_2CH_3$), 3.53–3.60 (m, 4H, $NCH_2(CH_2)_2CH_3$), 7.10–7.60 (m, 3H, *Ar*), 7.77 (d, 1H, *J* = 7.80 Hz, *Ar*), 8.06 (d, 1H, *J* = 7.20 Hz, *Ar*), 8.24 (d, 1H, *J* = 7.80 Hz, *Ar*), 11.30 (br, 1H, N*H*). ^{13}C NMR (DMSO-d_6): 160.23 (C=O), 155.65 (C10a), 153.36 (C3), 150.11 (C11a), 148.65 (C4a), 145.06 (C6b), 126.50 (C6), 125.89 (C9), 123.40 (C8), 123.31 (C7), 119.89 (C5), 116.82 (C10), 111.66 (C11b), 103.50 (C6a), 46.89 ($2CH_2$), 29.70 ($2CH_2$), 19.44 ($2CH_2$), 13.87 ($2CH_3$). MS (ESI^+): 364 (M^+ +1). Anal. Calcd for $C_{22}H_{25}N_3O_2$: C, 72.70; H, 6.93; N, 11.56. Found: C, 72.73; H, 6.89; N, 11.53.

*4.1.1.6. 3-(Pyrrolidin-1-yl)benzofuro[2,3-f]quinazolin-1(2H)-one (**9**).* White powder (40% yield). Mp > 260 °C. IR (KBr) (cm^{-1}): 3448 (ν NH), 3043 (CH arom.), 2952 (ν CH aliph.), 1681 (ν C=O), 1598 (ν C=C), 1462 (ν C=C), 1191, 832, 743. ^{1}H NMR (DMSO-d_6): δ 1.79–1.89 (t, 4H, CH_2 pyrrolidine), 3.42–3.47 (t, 4H, NCH_2 pyrrolidine), 7.19 (d, 1H, *J* = 8.55 Hz, *Ar*), 7.27–7.40 (m, 2H, *Ar*), 7.69 (d, 1H, *J* = 7.86 Hz, *Ar*), 7.90 (dd, 1H, J_1 = 8.63 Hz, J_2 = 1.35 Hz, *Ar*), 8.18 (d, 1H, *J* = 8.53 Hz, *Ar*), 11.10 (br, 1H, N*H*). ^{13}C NMR (DMSO-d_6): 161. 21 (C=O), 156. 53 (C10a), 155.65 (C3), 153.51 (C11a), 148.67 (C4a), 146.45 (C6b), 130.87 (C6), 126.34 (C9), 123.45 (C8), 123.56 (C7), 120.04 (C5), 119.87 (C10), 112.21 (C11b), 101.34 (C6a), 58.42 ($2CH_2$), 23.21 ($2CH_2$). MS (ESI^+): 306 (M^+ +1). Anal. Calcd for $C_{18}H_{15}N_3O_2$: C, 70.81; H, 4.95; N, 13.76. Found: C, 70.84; H, 4.92; N, 13.80.

*4.1.1.7. 3-(Morpholin-1-yl)benzofuro[2,3-f]quinazolin-1(2H)-one (**10**).* White powder (51% yield). Mp > 260 °C. IR (KBr) (cm^{-1}): 3452 (ν NH), 3108 (CH arom.), 2968 (ν CH aliph.), 1671 (ν C=O), 1588 (ν C=C), 1452 (ν C=C), 1181, 1118, 1004, 889, 743. ^{1}H NMR (DMSO-d_6): δ 3.68–3.80 (m, 8H, CH_2 morpholine), 7.38–7.53 (m, 3H, *Ar*), 7.78 (d, 1H, *J* = 8.10 Hz, *Ar*), 8.04 (d, 1H, *J* = 8.70 Hz, *Ar*), 8.32 (d, 1H, *J* = 8.40 Hz, *Ar*), 11.55 (br, 1H, N*H*). ^{13}C NMR (DMSO-d_6): 161.32 (C=O), 157.21 (C10a), 155.32 (C3), 153.22 (C11a), 149.11 (C4a), 146.76 (C6b), 130.21 (C6), 126.45 (C9), 123.56 (C8), 123.45 (C7), 120.67 (C5), 119.56 (C10), 112.45 (C11b), 103.10 (C6a), 65.21 ($2CH_2$), 58.70 ($2CH_2$). MS (ESI^+): 322 (M^+ +1). Anal. Calcd for $C_{18}H_{15}N_3O_3$: C, 67.28; H, 4.71; N, 13.38. Found: C, 67.31; H, 4.74; N, 13.36.

*4.1.1.8. 3-(Piperidin-1-yl)benzofuro[2,3-f]quinazolin-1(2H)-one (**11**).* White powder (38% yield). Mp > 260 °C. IR (KBr) (cm^{-1}): 3421 (ν NH), 3056 (ν CH arom.), 2932 (ν CH aliph.), 1671 (ν C=O), 1588 (ν C=C), 1462 (ν C=C), 1259, 1176, 837, 749. ^{1}H NMR (DMSO-d_6): δ 1.10–1.15 (m, 2H, CH_2 piperidine), 1.40–1.55 (m, 4H, CH_2 piperidine), 3.58–3.61 (m, 4H, NCH_2 piperidine), 7.18 (d, 1H, *J* = 8.58 Hz, *Ar*), 7.28–7.42 (m, 2H, *Ar*), 7.70 (d, 1H, *J* = 7.75 Hz, *Ar*), 8.01 (d, 1H, *J* = 7.62 Hz, *Ar*), 8.20 (d, 1H, *J* = 8.47 Hz, *Ar*), 11.30 (br, 1H, N*H*). ^{13}C NMR (DMSO-d_6): 159.56 (C=O), 156.13 (C10a), 155.65 (C3), 153.40 (C11a), 147.32 (C4a), 145.32 (C6b), 127.44 (C6), 126.37 (C9), 123.32 (C8), 121.15 (C7), 119.97 (C5), 117.27 (C10), 111.65 (C11b), 103.53 (C6a), 45.65 ($2CH_2$), 25.17 ($2CH_2$), 23.95 (CH_2). MS (EI) *m/z* (%): 319 ($M^{+\cdot}$, 100), 290 (100). MS (ESI^+): 320 (M^+ +1). Anal. Calcd for $C_{19}H_{17}N_3O_2$: C, 71.46; H, 5.37; N, 13.16. Found: C, 71.44; H, 5.40; N, 13.19.

*4.1.1.9. 3-(Diethylamino)-5-methoxybenzofuro[2,3-f]quinazolin-1(2H)-one (**12**).* Yellow powder (55% yield). Mp > 260 °C. IR (KBr) (cm^{-1}): 3412 (ν NH), 2971 (ν CH aliph.), 1659 (ν C=O), 1598 (ν C=C), 1443 (ν C=C), 1353, 1173, 1056, 1019, 845, 738. ^{1}H NMR (DMSO-d_6): δ 1.12–1.18 (m, 6H, CH_3), 3.60–3.67 (m, 4H, CH_2CH_3), 3.90 (s, 3H, OCH_3), 7.26–7.50 (m, 2H, *Ar*), 7.70 (d, 1H, *J* = 8.28 Hz, *Ar*), 7.87 (s, 1H, *Ar*), 8.07 (d, *J* = 8.56 Hz, 1H, *Ar*), 10.30 (br, 1H, N*H*). ^{13}C NMR (DMSO-d_6): 161.01 (C=O), 155.56 (C10a), 149.35 (11a), 148.58 (C3), 147.59 (C5), 129.21 (C6b), 125.21 (C4a), 123.95 (C9), 122.98 (C8), 119.87 (C7), 115.36 (C10), 111.59 (C11b), 107.30 (C6a), 103.55 (C6), 56.75 (OCH_3), 42.21 ($2CH_2$), 13.20 ($2CH_3$). MS (EI) *m/z* (%): 337 ($M^{+\cdot}$, 100), 308 (100) ($M^{+\cdot} - CH_2CH_3$), Anal. Calcd for $C_{19}H_{19}N_3O_3$: C, 67.64; H, 5.68; N, 12.45. Found: C, 67.69; H, 5.65; N, 12.48.

*4.1.1.10. 3-(Dipropylamino)-5-methoxybenzofuro[2,3-f]quinazolin-1(2H)-one (**13**).* Yellow powder (60% yield). Mp = 254 °C. IR (KBr) (cm^{-1}): 3146 (ν NH), 3055 (ν CH arom.), (2961 (ν CH aliph.), 1665 (ν

C=O), 1586 (ν C=C), 1460 (ν C=C), 1270 (ν_{as} = C–O–C), 1106 (ν_s = C–O–C), 745, 721. ^{1}H NMR (DMSO-d_6): δ 0.88–0.92 (t, 6H, CH_2CH_3), 1.56–1.65 (m, 4H, $CH_2CH_2CH_3$), 3.51–3.55 (m, 4H, $NCH_2CH_2CH_3$), 3.95 (s, 3H, OCH_3), 7.35–7.44 (m, 2H, *Ar*), 7.73 (d, 1H, *J* = 8.40 Hz, *Ar*), 7.88 (s, 1H, *Ar*), 8.07 (d, 1H, *J* = 7.60 Hz, *Ar*), 11.36 (br, 1H, N*H*). ^{13}C NMR (DMSO-d_6): 161.35 (C=O), 156.00 (C10a), 150.33 (C11a), 149.86 (C3), 148.11 (C5), 144.17 (C6b), 125.99 (C4a), 124.37 (C9), 123.39 (C8), 120.28 (C7), 115.71 (C10), 112.02 (C11b), 108.25 (C6), 103.96 (C6a), 57.41 (OCH_3), 49.21 ($2CH_2$), 21.18 ($2CH_2$), 11.49 ($2CH_3$). MS (EI) *m/z* (%): 365 ($M^{+\cdot}$, 100), 322 (50) ($M^{+\cdot} - CH_2CH_2CH_3$), 294 (100). MS ($ESI^+$): 366 ($M^+ +1$). Anal. Calcd for $C_{21}H_{23}N_3O_3$: C, 69.02; H, 6.34; N, 11.50. Found: C, 69.04; H, 6.31; N, 11.53.

*4.1.1.11. 3-(Dibutylamino)-5-methoxybenzofuro[2,3-f]quinazolin-1(2H)-one (**14**).* Yellow powder (70% yield). Mp = 196 °C. IR (KBr) (cm^{-1}): 3126 (ν NH), 3050 (ν CH arom.), 2955 (ν CH aliph.), 1656 (ν C=O), 1599 (ν C=C), 1462 (ν C=C), 1187, 1052, 799, 740, 556. ^{1}H NMR ($CDCl_3$): δ 0.80–0.97 (m, 6H, CH_3), 1.25–1.48 (m, 4H, CH_2CH_3), 1.51–1.90 (m, 4H, $CH_2CH_2CH_3$), 3.60–3.80 (m, 4H, NCH_2), 3.95 (s, 3H, OCH_3), 7.25–7.40 (m, 2H, *Ar*), 7.50 (s, 1H, *Ar*), 7.60 (d, 1H, *J* = 8.10 Hz, *Ar*), 7.80 (d, 1H, *J* = 7.20 Hz, *Ar*), 9.42 (br, 1H, N*H*). ^{13}C NMR (DMSO-d_6): 161.02 (C=O), 155.51 (C10a), 149.85 (C11a), 149.38 (C3), 147.56 (C5), 127.93(C6b), 125.52 (C4a), 123.91 (C9), 122.91(C8), 119.80 (C7), 115.27 (C10), 111.56 (C11b), 107.57 (C6), 103.44 (C6a), 56.85 (OCH_3), 46.41 ($2CH_2$), 27.48 ($2CH_2$), 19.30 ($2CH_2$), 13.51 ($2CH_3$). MS (EI) *m/z* (%): 393 ($M^{+\cdot}$, 77), 294 (100). MS (ESI^+): 394 ($M^+ +1$). Anal. Calcd for $C_{23}H_{27}N_3O_3$: C, 70.21; H, 6.92; N, 10.68. Found: C, 70.24; H, 6.89; N, 10.71.

*4.1.1.12. 5-Methoxy-3-(pyrrolidin-1-yl)benzofuro[2,3-f]quinazolin-1(2H)-one (**15**).* White powder (54% yield). Mp > 260 °C. IR (KBr) (cm^{-1}): 3432 (ν NH), 2955 (ν CH aliph.), 1681 (ν C=O), 1599 (ν C=C), 1466 (ν C=C), 1355, 1193, 1060, 740, 555. ^{1}H NMR (DMSO-d_6): δ 1.90–1.93 (m, 4H, CH_2 pyrrolidine), 3.53–3.55 (m, 4H, CH_2–N–CH_2 pyrrolidine), 3.94 (s, 3H, OCH_3), 7.35–7.41 (m, 2H, *Ar*), 7.70 (d, 1H, *J* = 8.32 Hz, *Ar*), 7.85 (s, 1H, *Ar*), 8.04 (d, 1H, *J* = 7.08 Hz, *Ar*), 11.30 (br, 1H, N*H*). ^{13}C NMR (DMSO-d_6): 161.11 (C=O), 155.49 (C10a), 149.75 (C11a), 149.43 (C3), 147.48 (C5), 128.05 (C6b), 125.36 (C4a), 123.87 (C9), 123.21 (C8), 119.98 (C7), 115.29 (C10), 111.54 (C11b), 107.58 (C6), 103.54 (C6a), 56.42 (OCH_3), 49.05 ($2CH_2$), 24.87 ($2CH_2$). MS (EI) *m/z* (%): 335 ($M^{+\cdot}$, 100), 320 (25) ($M^{+\cdot} - CH_3$). MS (ESI^+): 336 ($M^+ +1$). Anal. Calcd for $C_{19}H_{17}N_3O_3$: C, 68.05; H, 5.11; N, 12.53. Found: C, 68.01; H, 5.08; N, 12.56.

*4.1.1.13. 5-Methoxy-3-(morpholin-1-yl)benzofuro[2,3-f]quinazolin-1(2H)-one (**16**).* White powder (40% yield). Mp > 260 °C. IR (KBr) (cm^{-1}): 3435 (ν NH), 2956 (ν CH aliph.), 1678 (ν C=O), 1587 (ν C=C), 1451 (ν C=C), 1261, 1169, 1117, 1061, 1010, 872, 744, 556. ^{1}H NMR (DMSO-d_6): δ 3.60–3.75 (m, 8H, CH_2 morpholine), 3.95 (s, 3H, OCH_3), 7.35–7.50 (m, 2H, *Ar*), 7.75 (d, 1H, *J* = 8.28 Hz, *Ar*), 7.95 (s, 1H, *Ar*), 8.10 (d, 1H, *J* = 8.56 Hz, *Ar*), 11.20 (br, 1H, N*H*). ^{13}C NMR (DMSO-d_6): 161.13 (C=O), 155.54 (C10a), 149.86 (C11a), 149.32 (C3), 147.56 (C5), 134.32 (C6b), 125.45 (C4a), 124.12 (C9), 123.76 (C8), 120.76 (C7), 115.76 (C10), 111.89 (C11b), 108.21 (C6), 103.78 (C6a), 56.54 (OCH_3), 65.05 ($2CH_2$), 57.23 ($2CH_2$). MS (EI) *m/z* (%): 351 ($M^{+\cdot}$, 100). MS (ESI^+): 352 ($M^+ +1$). Anal. Calcd for $C_{19}H_{17}N_3O_4$: C, 64.95; H, 4.88; N, 11.96. Found: C, 64.92; H, 4.90; N, 12.00.

*4.1.1.14. 5-Methoxy-3-(piperidin-1-yl)benzofuro[2,3-f]quinazolin-1(2H)-one (**17**).* Yellow powder (83% yield). Mp > 260 °C. IR (KBr) (cm^{-1}): 2941 (ν CH aliph.), 2841 (ν CH aliph.), 1678 (ν C=O), 1586 (ν C=C), 1463 (ν C=C), 1353, 1232, 1058, 798, 739, 555. ^{1}H NMR (DMSO-d_6): δ 1.47–1.70 (m, 6H, CH_2 piperidine), 2.93–3.02 (m, 4H, H_2C–N–CH_2 piperidine), 3.96 (s, 3H, OCH_3), 7.32–7.50 (m, 2H, *Ar*), 7.75 (d, 1H, *J* = 8.28 Hz, *Ar*), 7.92 (s, 1H, *Ar*), 8.10 (d, 1H, *J* = 8.56 Hz, *Ar*), 9.80 (br, 1H, N*H*). ^{13}C NMR (DMSO-d_6): 160.23 (C=O), 155.61 (C10a), 149.43 (C11a), 149.12 (C3), 147.34 (C5), 128.31 (C6b), 125.63 (C4a), 123.85 (C9), 122.89 (C8), 119.83 (C7), 115.84 (C10), 111.48 (C11b), 107.37 (C6), 104.32 (C6a), 60.02 ($2CH_2$), 56.71 (OCH_3), 25.17 ($2CH_2$), 23.91 (CH_2). MS (EI) *m/z* (%): 349 ($M^{+\cdot}$, 100), 334 (27) ($M^{+\cdot} - CH_3$). MS (ESI^+): 350 ($M^+ +1$). Anal. Calcd for $C_{20}H_{19}N_3O_3$: C, 68.75; H, 5.48; N, 12.03. Found: C, 68.78; H, 5.51; N, 11.99.

*4.1.2. 3-(Dipropylamino)-5-hydroxy-benzofuro[2,3-f]quinazolin-1(2H)-one (**18, DPA-HBFQ-1**)*

A mixture of 3-dipropyl-5-methoxybenzofuro[2,3-*f*]quinazolin-1(2*H*)-one **(13)** (1.37 mmol, 0.50 g) and anhydrous pyridine hydrochloride (6.85 mmol, 0.79 g) was heated to reflux for 2h. The reaction mixture was left to cool to room temperature, and then ice-cold water was added. The product was extracted with Et_2O (50 mL). The organic layers were washed with an aqueous solution of HCl (2N), dried ($MgSO_4$) and concentrated to give green powder (30% yield). Mp > 260 °C. IR (KBr) (cm^{-1}): 3390 (ν O–H), 3182 (ν NH), 2931 (ν CH aliph.), 1668 (ν C=O), 1355, 1177, 1029, 744. ^{1}H NMR (DMSO-d_6): δ 0.89–0.97 (t, 6H, CH_3), 1.54–1.63 (m, 4H, $CH_2CH_2CH_3$), 3.57–3.61 (m, 4H, $CH_2CH_2CH_3$), 7.33–7.43 (m, 2H, *Ar*), 7.71–7.73 (m, 2H, *Ar*), 8.02 (d, 1H, J = 7.36 Hz, *Ar*), 8.23 (br, 1H, O*H*), 11.33 (br, 1H, N*H*). ^{13}C NMR (DMSO-d_6): 161.25 (C=O), 155.96 (C10a), 150.49 (C11a), 146.90 (C3), 146.52 (C5), 141.53 (C6b), 126.04 (C4a), 124.31 (C9), 123.31(C8), 120.37 (C7), 116.18 (C11b), 111.98 (C10), 107.85 (C6), 102.99 (C6a), 49.01 ($2CH_2$), 21.15 ($2CH_2$), 11.44 ($2CH_3$). MS (EI) *m/z* (%): 351 ($M^{+\cdot}$, 100), 278 (78). Anal. Calcd for $C_{20}H_{21}N_3O_3$: C, 68.36; H, 6.02; N, 11.96. Found: C, 68.32; H, 6.05; N, 11.93.

4.2. Biological methods

Dulbecco's Modified Eagle's Medium/Nutrient Mixture F-12 Ham, DMEM, Minimum Essential Medium, MEM, Ham's F-10 Nutrient Mixture, 100 bp DNA ladder, L-Glutamine, penicillin, streptomycin, bovine serum albumine, phosphate-buffered saline were purchased from Invitrogen (Carlsbad, CA,USA), Dual luciferase kit, FuGENE 6, CMV renilla luciferase plasmid was provided by Promega (Madison, WI, USA). The RETROscript kit and DNase I were purchased from Ambion (Austin, TX, USA). Aprotinin, leupeptin, phenylmethylsulfonyl fluoride, sodium orthovanadate, formaldehyde, NP-40, MTT, dimethyl sulphoxide, by Sigma (Milan, Italy). ECL System, antibodies against p53, p21, GAPDH and beta-actin were provided by Santa Cruz Biotechnology (Santa Cruz, CA, USA), Triazol, SYBR Green Universal PCR Master Mix by Biosystems (Forster City, CA, USA). Human Topoisomerase I and II, pHOT1 and kDNA were purchased from TopoGEN (Port Orange, FL).

4.2.1. Cell cultures

All the cell lines used in these studies (with the exception of MCF-7 TR1) were acquired from American Type Culture Collection (ATCC, Manassas, VA) where they were authenticated, stored according to supplier's instructions, and used within a months after frozen aliquots resuscitations. MCF-7 cells were cultured in DMEM-F12 containing 10% fetal bovine serum (FBS), 1% L-Glutamine, 1 mg/mL penicillin–streptomycin. MCF-10A normal breast epithelial cells were grown in DMEM-F12 plus glutamax containing 5% horse serum (Invitrogen Carlsbad, CA, US), 1 mg/mL penicillin–streptomycin, 0.5 mg/mL hydrocortisone, and 10 mg/mL insulin. MDA-MB-231 cells were cultured in DMEM containing 5% FBS, 1% L-Glutamine, 1 mg/mL penicillin–streptomycin. Every 4 months cells were authenticated by single tandem repeat analysis at our Sequencing Core, morphology, doubling times, estrogen sensitivity, and mycoplasma negativity were tested (MycoAlert,

Lonza). MCF-7 TR1 cells were generated in the laboratory of Dr. Fuqua as previously described [56] and maintained with 10^{-6} M of 4-hydroxytamoxifen. R2C cells were cultured in Ham's F-10 nutrient mix containing 15% Horse serum, 2.5% FBS, 1% L-Glutamine and 1 mg/mL penicillin–streptomycin. Ishikawa and HeLa cells were cultured in MEM containing 10% FBS, 1% L-Glutamine, 1% NEAA, and 1 mg/mL penicillin–streptomycin. HepG2 cells were cultured in DMEM containing 10% FBS, 1% L-Glutamine and 1 mg/mL penicillin–streptomycin.

4.2.2. Plasmids

The human wild-type $p21^{Cip1/WAF1}$ promoter-luciferase (luc) reporter (WT) and its deletion construct that lacks the two p53-binding sites (Δp53) were kind gifts from Dr. T. Sakai (Kyoto Prefectural University of Medicine, Kyoto, Japan).

4.2.3. Western blot analysis

Cells were treated as indicated before lysis. Equal amounts of cell extracts were subjected to SDS-PAGE, as described [57,58] Blots are representative of at least three independent experiments.

4.2.4. Real-time RT-PCR

The gene expression of p53, p21 and GAPDH was evaluated by real-time RT-PCR. Total RNA was reverse transcribed with RETROscript kit. 5 μl of diluted (1:3) cDNA was analyzed in triplicate by real-time PCR in an iCycler iQ Detection System (Bio-Rad) using SYBR Green Universal PCR Master Mix, following the manufacturer's recommendations. Each sample was normalized on its GAPDH mRNA content. Primers used for the amplification were: forward 5′-CCGTGTTGGTTCATCCCTGTA-3′ and reverse 5′-TTTTGGATTTTTAAGACAGAGTCTTTGTA-3′(p53); forward 5′-GCATGACAGATTTCTACCACTCC-3′ and reverse 5′-AAGATGTAGAGCGGGCCTTT-3′(p21); forward 5′-CCCACTCCTCCACCTTTGAC-3′ and reverse 5′-TGTTGCTGTAGCCAAATTCGTT-3′ (GAPDH). The relative gene expression levels were calculated as described [59,60].

4.2.5. Clonogenic assay

MCF-7 (1000 cells/plate) or MCF-7 TR-1 (1000 cells/plate) cells were plated in 12-multiwell plates. After an overnight incubation, cells were treated with 100 μM of **DPA-HBFQ-1** for 24 h. Cells were then washed, and fresh media were added. After 14 days of incubation, surviving colonies were fixed and stained with Crystal Violet stain. Experiments were repeated, and data are representative of replicate experiments.

4.2.6. DNA fragmentation

Cells were collected and washed with PBS and pelleted at 1800 rpm for 5 min. The samples were resuspended in 0.5 mL of extraction buffer (50 mmol/L Tris–HCl, pH 8; 10 mmol/L EDTA, 0.5% SDS) for 20 min in rotation at 48C. DNA was extracted three times with phenol-chloroform and one time with chloroform. The aqueous phase was used to precipitate nucleic acids with 0.1 volumes of 3M sodium acetate and 2.5 volumes cold ethanol overnight at −20 °C. The DNA pellet was resuspended in 15 μL H_2O treated with RNase A for 30 min at 37 °C. The extracted DNA was subjected to electrophoresis on 1.5% agarose gels, stained with ethidium bromide and then photographed.

4.2.7. Transient transfection assays

MCF-7 cells were transiently transfected using the FuGENE 6 reagent with p53 or p21 gene promoter, different deleted segments, and treated as indicated. Empty vectors were used to ensure that DNA concentrations were constant in each transfection. Luciferase activities were assayed using Dual Luciferase assay system (Promega) [61,62].

4.2.8. RNA interference (RNAi)

MCF-7 cells were transfected with RNA duplex of stealth RNA interference (RNAi)-targeted for human p53 mRNA sequence 5′-GCCAAGUCUGUGACUUGCACGUACU -3′ (Life Science) or with a stealth RNAi-negative control (Life Science) to a final concentration of 100 nM using Lipofectamine 2000 as recommended by the manufacturer [63,64].

4.2.9. Cell proliferation assays

Cell proliferation was determined by using 3-(4,5-dimethylthiazol-2-yl)-2,5-diphenylformazan (MTT) assay as described [65–68] Data are representative of three independent experiments, each performed in triplicate. The IC_{50} values were calculated using GraphPad Prism 4 (GraphPad Software, Inc., San Diego, CA) as described [69–71].

4.2.10. Soft agar anchorage-independent growth assays

Cells (104/well) were plated in 4 mL of 0.35% agarose with 5% charcoal stripped-FBS in phenol red-free media, with a 0.7% agarose base in six well plates. Two days after plating, media containing vehicle or treatments as indicated were added to the top layer, and replaced every 2 days. After 14 days, 300 mL of MTT was added to each well and allowed to incubate at 37 °C for 4 h. Plates were then placed at 4 °C overnight and colonies >50 mm diameter from triplicate assays were counted. The data are representative of three independent experiments, each performed in triplicate [72,73].

4.2.11. Human Topoisomerase I relaxation assay

Relaxation assays were performed in a final volume of 20 μL and assembled as follows. 0.25 μg of supercoiled pHOT1 in TE buffer [TE: 10 mM Tris-HCl (pH 7.5), 1 mM EDTA] (TopoGEN, Port Orange, FL) was added to a solution containing water (variable volume) and 1X assay buffer (10 mM Tris-HCl (pH 7.9), 1 mM EDTA, 0.5 mM NaCl, 0.1% bovine serum albumin, 0.1 mM spermidine and 5% glycerol). Next, the compounds to be tested were added and the reaction initiated by addition of recombinant human topo I (2 U) (TopoGEN, Port Orange, FL). The reactions were incubated at 37 °C for 30 min and terminated by the addition of 5 × stop buffer (5% sarkosyl, 25% glycerol, 0.125% bromophenol blue). Samples underwent to Proteinase K digestion (50 μg/mL) at 37 °C for 30 min, followed by extraction with an equal volume of chloroform:isoamylic alcohol (24:1), vortexed and centrifuged for 30 s. The upper aqueous phase was withdrawn, loaded onto a 1% agarose gel containing 1X TAE buffer (diluted from 50X buffer containing 242 g Tris base, 57.1 mL glacial acetic acid and 100 mL of 0.5 M EDTA) without ethidium bromide (EB). After the run, agarose gel was colored with 1X TAE buffer containing EB (0.5 μg/mL) for 30 min and destained with distilled water for 15 min, then visualized using a UV transilluminator.

4.2.12. Human Topoisomerase II decatenation assay

Decatenation assays were performed in a final volume of 20 μL, as follows. 0.3 μg of kinetoplast DNA (kDNA) (topoGEN, Port Orange, FL) were added to a solution containing water, 1X assay buffer [which contains: 50 mM Tris-HCl, pH of 8, 150 mM NaCl, 10 mM $MgCl_2$, 0.5 mM Dithiothreitol (DTT) and 30 μg/mL bovine serum albumin (BSA)], and 1 mM ATP. The compounds to be tested were added and the reaction started by the addition of 3 U of human topoisomerase II (topoGEN, Port Orange, FL) and incubated at 37 °C for 30 min. At the end, 5X stop buffer has been added and the samples were treated as described in the previous paragraph. The aqueous phase has been loaded on a 1% agarose gel containing 1X TAE buffer with EB (0.5 μg/mL) and visualized using an UV

transilluminator.

4.2.13. Statistical analysis

Data were analyzed for statistical significance ($P < 0.05$) using One-way ANOVA followed by Dunnett's test performed by Graph Pad Prism 4. Standard deviations (SD) are shown.

Acknowledgment

This work was supported by Commissione Europea, Fondo Sociale Europeo (FSE 2007/2013-PROGRAMMA ARUE) and Regione Calabria to Domenico Iacopetta.

Appendix A. Supplementary data

Supplementary data related to this article can be found at http://dx.doi.org/10.1016/j.ejmech.2015.11.004.

References

[1] A. Jemal, F. Bray, M.M. Center, J. Ferlay, E. Ward, D. Forman, Global cancer statistics, CA Cancer J. Clin. 61 (2011) 69–90.
[2] D.M. Parkin, F. Bray, J. Ferlay, P. Pisani, Global cancer statistics, 2002, CA Cancer J. Clin. 55 (2005) 74–108.
[3] A. Chimento, M. Sala, I.M. Gomez-Monterrey, S. Musella, A. Bertamino, A. Caruso, M.S. Sinicropi, R. Sirianni, F. Puoci, O.I. Parisi, C. Campana, E. Martire, E. Novellino, C. Saturnino, P. Campiglia, V. Pezzi, Biological activity of 3-chloro-azetidin-2-one derivatives having interesting antiproliferative activity on human breast cancer cell lines, Bioorg. Med. Chem. Lett. 23 (2013) 6401–6405.
[4] O.I. Parisi, C. Morelli, F. Puoci, C. Saturnino, A. Caruso, D. Sisci, G.E. Trombino, N. Picci, M.S. Sinicropi, Magnetic molecularly imprinted polymers (MMIPs) for carbazole derivative release in targeted cancer therapy, J. Mater. Chem. B 2 (2014) 6619–6625.
[5] E. Chosson, F. Santoro, C. Rochais, J.S.D. Santos, R. Legay, S. Thoret, T. Cresteil, M.S. Sinicropi, T. Besson, P. Dallemagne, Synthesis of novel 7-oxo and 7-hydroxy trifluoroallocolchicinoids with cytotoxic effect, Bioorg. Med. Chem. 20 (2012) 2614–2623.
[6] C. Saturnino, C. Palladino, M. Napoli, M.S. Sinicropi, A. Botta, M. Sala, A. Carcereri de Prati, E. Novellino, H. Suzuki, Synthesis and biological evaluation of new N-alkylcarbazole derivatives as STAT3 inhibitors: preliminary study, Eur. J. Med. Chem. 60 (2013) 112–119.
[7] E. Moustacchi, DNA damage and repair: consequences on dose-responses, Mutat. Res. 464 (2000) 35–40.
[8] J. Blasiak, M. Arabski, R. Krupa, K. Wozniak, J. Rykala, A. Kolacinska, Z. Morawiec, J. Drzewoski, M. Zadrozny, Basal, oxidative and alkylative DNA damage, DNA repair efficacy and mutagen sensitivity in breast cancer, Mutat. Res. 554 (2004) 139–148.
[9] S. Madhusudan, M.R. Middleton, The emerging role of DNA repair proteins as predictive, prognostic and therapeutic targets in cancer, Cancer Treat. Rev. 31 (2005) 603–617.
[10] S. Madhusudan, I.D. Hickson, DNA repair inhibition: a selective tumour targeting strategy, Trends Mol. Med. 11 (2005) 503–511.
[11] L.F.Z. Batista, W.P. Roos, M. Christmann, C.F.M. Menck, B. Kaina, Differential sensitivity of malignant glioma cells to methylating and chloroethylating anticancer drugs: p53 determines the switch by regulating xpc, ddb2, and DNA double-strand breaks, Cancer Res. 67 (2007) 11886–11895.
[12] A. Caruso, A. Sophie Voisin-Chiret, J.C. Lancelot, M.S. Sinicropi, A. Garofalo, S. Rault, Novel and efficient synthesis of 5,8-dimethyl-9h-carbazol-3-ol via a hydroxydeboronation reaction, Heterocycles 71 (2007) 2203–2210.
[13] J.F. Lohier, A. Caruso, J.D. Santos, J.C. Lancelot, S. Rault, tert-Butyl 6-bromo-1,4-dimethyl-9H-carbazole-9-carboxylate, Acta Crystallogr. Sect. E Struct. Rep. Online 66 (2010). O1971–U1791.
[14] A. Panno, M.S. Sinicropi, A. Caruso, H. El-Kashef, J.-C. Lancelot, G. Aubert, A. Lesnard, T. Cresteil, S. Rault, New Trimethoxybenzamides and Trimethoxyphenylureas derived from Dimethylcarbazole as cytotoxic agents. Part I, J. Heterocycl. Chem. 51 (2014) 294–302.
[15] S. Goodwin, A.F. Smith, E.C. Horning, Alkaloids of ochrosia elliptica Labill, J. Am. Chem. Soc. 81 (1959) 1903–1908.
[16] M. Hagg, M. Berndtsson, A. Mandic, R. Zhou, M.C. Shoshan, S. Linder, Induction of endoplasmic reticulum stress by ellipticine plant alkaloids, Mol. Cancer Ther. 3 (2004) 489–497.
[17] C. Asche, M. Demeunynck, Antitumor carbazoles, Anticancer Agents Med. Chem. 7 (2007) 247–267.
[18] S.L. Pandrangi, R. Chikati, P.S. Chauhan, C.S. Kumar, A. Banarji, S. Saxena, Effects of ellipticine on ALDH1A1-expressing breast cancer stem cells–an in vitro and in silico study, Tumour Biol. 35 (2014) 723–737.
[19] J. Sopkova-de Oliveira Santos, A. Caruso, J.F. Lohier, J.C. Lancelot, S. Rault, 9-Ethyl-1,4-dimethyl-6-(4,4,5,5-tetramethyl-1,3,2-dioxaborolan-2-yl)-9H-carbazole and 6-bromo-9-ethyl-1,4-dimethyl-9H-carbazole, Acta Crystallogr. C 64 (2008) o453–455.
[20] A. Caruso, A.S. Voisin-Chiret, J.C. Lancelot, M.S. Sinicropi, A. Garofalo, S. Rault, Efficient and simple synthesis of 6-aryl-1,4-dimethyl-9H-carbazoles, Molecules 13 (2008) 1312–1320.
[21] M. Stiborova, E. Frei, Ellipticines as DNA-targeted chemotherapeutics, Curr. Med. Chem. 21 (2014) 575–591.
[22] N.C. Garbett, D.E. Graves, Extending nature's leads: the anticancer agent ellipticine, Curr. Med. Chem. Anticancer Agents 4 (2004) 149–172.
[23] M. Stiborova, M. Rupertova, H.H. Schmeiser, E. Frei, Molecular mechanisms of antineoplastic action of an anticancer drug ellipticine, Biomed. Pap. Med. Fac. Univ. Palacky. Olomouc Czech. Repub. 150 (2006) 13–23.
[24] M. Stiborova, C.A. Bieler, M. Wiessler, E. Frei, The anticancer agent ellipticine on activation by cytochrome P450 forms covalent DNA adducts, Biochem. Pharmacol. 62 (2001) 1675–1684.
[25] M. Stiborova, M. Rupertova, E. Frei, Cytochrome P450- and peroxidase-mediated oxidation of anticancer alkaloid ellipticine dictates its anti-tumor efficiency, Biochim. Biophys. Acta 1814 (2011) 175–185.
[26] M. Stiborova, J. Poljakova, E. Martinkova, L. Borek-Dohalska, T. Eckschlager, R. Kizek, E. Frei, Ellipticine cytotoxicity to cancer cell lines - a comparative study, Interdiscip. Toxicol. 4 (2011) 98–105.
[27] R. Kizek, V. Adam, J. Hrabeta, T. Eckschlager, S. Smutny, J.V. Burda, E. Frei, M. Stiborova, Anthracyclines and ellipticines as DNA-damaging anticancer drugs: recent advances, Pharmacol. Ther. 133 (2012) 26–39.
[28] R. Jasztold-Howorko, B. Tylinska, B. Biadun, T. Gebarowski, K. Gasiorowski, New pyridocarbazole derivatives. Synthesis and their in vitro anticancer activity, Acta Pol. Pharm. 70 (2013) 823–832.
[29] A. Caruso, M.S. Sinicropi, J.C. Lancelot, H. El-Kashef, C. Saturnino, G. Aubert, C. Ballandonne, A. Lesnard, T. Cresteil, P. Dallemagne, S. Rault, Synthesis and evaluation of cytotoxic activities of new guanidines derived from carbazoles, Bioorg. Med. Chem. Lett. 24 (2014) 467–472.
[30] A. Caruso, A. Chimento, H. El-Kashef, J.C. Lancelot, A. Panno, V. Pezzi, C. Saturnino, M.S. Sinicropi, R. Sirianni, S. Rault, Antiproliferative activity of some 1,4-dimethylcarbazoles on cells that express estrogen receptors: part I, J. Enzyme Inhib. Med. Chem. 27 (2012) 609–613.
[31] P.L. Kuo, Y.L. Hsu, C.H. Chang, C.C. Lin, The mechanism of ellipticine-induced apoptosis and cell cycle arrest in human breast MCF-7 cancer cells, Cancer Lett. 223 (2005) 293–301.
[32] Y.C. Kuo, P.L. Kuo, Y.L. Hsu, C.Y. Cho, C.C. Lin, Ellipticine induces apoptosis through p53-dependent pathway in human hepatocellular carcinoma HepG2 cells, Life Sci. 78 (2006) 2550–2557.
[33] Y. Peng, C. Li, L. Chen, S. Sebti, J. Chen, Rescue of mutant p53 transcription function by ellipticine, Oncogene 22 (2003) 4478–4487.
[34] A. Caruso, J. Lancelot, H. El-Kashef, M.S. Sinicropi, R. Legay, R. Lesnard, S. Rault, A rapid and versatile synthesis of novel pyrimido[5,4-b]carbazoles, Tetrahedron 65 (2009) 10400–10405.
[35] P.L. Kuo, Y.L. Hsu, Y.C. Kuo, C.H. Chang, C.C. Lin, The anti-proliferative inhibition of ellipticine in human breast mda-mb-231 cancer cells is through cell cycle arrest and apoptosis induction, Anticancer Drugs 16 (2005) 789–795.
[36] T.W. Moody, G. Czerwinski, N.I. Tarasova, C.J. Michejda, VIP-ellipticine derivatives inhibit the growth of breast cancer cells, Life Sci. 71 (2002) 1005–1014.
[37] R. Chaniyara, S. Tala, C.W. Chen, X.G. Zang, R. Kakadiya, L.F. Lin, C.H. Chen, S.I. Chien, T.C. Chou, T.H. Tsai, T.C. Lee, A. Shah, T.L. Su, Novel antitumor Indolizino[6,7-b]indoles with multiple Modes of Action: DNA Cross-Linking and Topoisomerase I and II inhibition, J. Med. Chem. 56 (2013) 1544–1563.
[38] E.G. Russell, E.C. O'Sullivan, C.M. Miller, J. Stanicka, F.O. McCarthy, T.G. Cotter, Ellipticine derivative induces potent cytostatic effect in acute myeloid leukaemia cells, Invest. New Drugs 32 (2014) 1113–1122.
[39] A. Caruso, D. Iacopetta, F. Puoci, A.R. Cappello, C. Saturnino, M.S. Sinicropi, Carbazole derivatives: a promising scenario for breast cancer treatment, Mini Rev. Med. Chem. (2015), http://dx.doi.org/10.2174/1389557515666150709111342 (Epub ahead of print).
[40] A. Caruso, J.-C. Lancelot, H. El-Kashef, A. Panno, M.S. Sinicropi, R. Legay, A. Lesnard, A. Lepailleur, S. Rault, Four partners, three-step, one-pot reaction for a library of new 2-alkyl(dialkyl)aminoquinazolin-4(3H)-ones, J. Heterocycl. Chem. 51 (2014) E282–E293.
[41] Y.C. Wu, J.C. Li, J.J. Wu, P. Morgan, X. Xu, F. Rancati, S. Vallese, L. Raveglia, R. Hotchandani, N. Fuller, J. Bard, K. Cunningham, S. Fish, R. Krykbaev, S. Tam, S.J. Goldman, C. Williams, T.S. Mansour, E. Saiah, J. Sypek, W. Li, Discovery of potent and selective matrix metalloprotease 12 inhibitors for the potential treatment of chronic obstructive pulmonary disease (COPD), Bioorg. Med. Chem. Lett. 22 (2012) 138–143.
[42] J. Rouesse, M. Spielmann, F. Turpin, T. Le Chevalier, M. Azab, J.M. Mondesir, Phase II study of elliptinium acetate salvage treatment of advanced breast cancer, Eur. J. Cancer 29A (1993) 856–859.
[43] A.U. Buzdar, G.N. Hortobagyi, L.T. Esparza, F.A. Holmes, J.S. Ro, G. Fraschini, B. Lichtiger, Elliptinium acetate in metastatic breast cancer–a phase II study, Oncology 47 (1990) 101–104.
[44] A. Gouyette, D. Huertas, J.P. Droz, J. Rouesse, J.L. Amiel, Pharmacokinetics of 2-methyl-9-hydroxyellipticinium acetate (NSC-264137) in cancer patients (phase I study), Eur. J. Cancer Clin. Oncol. 18 (1982) 1285–1292.
[45] J. Kattan, M. Durand, J.P. Droz, M. Mahjoubi, J.P. Marino, M. Azab, Phase I study of retelliptine dihydrochloride (SR 95325 B) using a single two-hour intravenous infusion schedule, Am. J. Clin. Oncol. 17 (1994) 242–245.

[46] E. Sirignano, C. Saturnino, A. Botta, M.S. Sinicropi, A. Caruso, A. Pisano, R. Lappano, M. Maggiolini, P. Longo, Synthesis, characterization and cytotoxic activity on breast cancer cells of new half-titanocene derivatives, Bioorg. Med. Chem. Lett. 23 (2013) 3458–3462.
[47] C. Saturnino, E. Sirignano, A. Botta, M.S. Sinicropi, A. Caruso, A. Pisano, R. Lappano, M. Maggiolini, P. Longo, New titanocene derivatives with high antiproliferative activity against breast cancer cells, Bioorg. Med. Chem. Lett. 24 (2014) 136–140.
[48] E. Sugikawa, T. Hosoi, N. Yazaki, M. Gamanuma, N. Nakanishi, M. Ohashi, Mutant p53 mediated induction of cell cycle arrest and apoptosis at G1 phase by 9-hydroxyellipticine, Anticancer Res. 19 (1999) 3099–3108.
[49] M. Ohashi, E. Sugikawa, N. Nakanishi, Inhibition of p53 protein phosphorylation by 9-hydroxyellipticine: a possible anticancer mechanism, Jpn. J. Cancer Res. 86 (1995) 819–827.
[50] M. Hollstein, K. Rice, M.S. Greenblatt, T. Soussi, R. Fuchs, T. Sorlie, E. Hovig, B. Smith-Sorensen, R. Montesano, C.C. Harris, Database of p53 gene somatic mutations in human tumors and cell lines, Nucleic Acids Res. 22 (1994) 3551–3555.
[51] W.S. el-Deiry, T. Tokino, V.E. Velculescu, D.B. Levy, R. Parsons, J.M. Trent, D. Lin, W.E. Mercer, K.W. Kinzler, B. Vogelstein, WAF1, a potential mediator of p53 tumor suppression, Cell 75 (1993) 817–825.
[52] W.S. el-Deiry, T. Tokino, T. Waldman, J.D. Oliner, V.E. Velculescu, M. Burrell, D.E. Hill, E. Healy, J.L. Rees, S.R. Hamilton, et al., Topological control of p21WAF1/CIP1 expression in normal and neoplastic tissues, Cancer Res. 55 (1995) 2910–2919.
[53] K.F. Macleod, N. Sherry, G. Hannon, D. Beach, T. Tokino, K. Kinzler, B. Vogelstein, T. Jacks, p53-dependent and independent expression of p21 during cell growth, differentiation, and DNA damage, Genes Dev. 9 (1995) 935–944.
[54] F.M. Deane, E.C. O'Sullivan, A.R. Maguire, J. Gilbert, J.A. Sakoff, A. McCluskey, F.O. McCarthy, Synthesis and evaluation of novel ellipticines as potential anticancer agents, Org. Biomol. Chem. 11 (2013) 1334–1344.
[55] F. Sottile, I. Gnemmi, S. Cantilena, W.C. D'Acunto, A. Sala, A chemical screen identifies the chemotherapeutic drug topotecan as a specific inhibitor of the B-MYB/MYCN axis in neuroblastoma, Oncotarget 3 (2012) 535–545.
[56] I. Barone, L. Brusco, G. Gu, J. Selever, A. Beyer, K.R. Covington, A. Tsimelzon, T. Wang, S.G. Hilsenbeck, G.C. Chamness, S. Ando, S.A. Fuqua, Loss of Rho GDIalpha and resistance to tamoxifen via effects on estrogen receptor alpha, J. Natl. Cancer Inst. 103 (2011) 538–552.
[57] S. Catalano, I. Barone, C. Giordano, P. Rizza, H. Qi, G. Gu, R. Malivindi, D. Bonofiglio, S. Ando, Rapid estradiol/ERalpha signaling enhances aromatase enzymatic activity in breast cancer cells, Mol. Endocrinol. 23 (2009) 1634–1645.
[58] I. Barone, C. Giordano, R. Malivindi, M. Lanzino, P. Rizza, I. Casaburi, D. Bonofiglio, S. Catalano, S. Ando, Estrogens and PTP1B function in a novel pathway to regulate aromatase enzymatic activity in breast cancer cells, Endocrinology 153 (2012) 5157–5166.
[59] S. Catalano, P. Rizza, G. Gu, I. Barone, C. Giordano, S. Marsico, I. Casaburi, E. Middea, M. Lanzino, M. Pellegrino, S. Ando, Fas ligand expression in TM4 Sertoli cells is enhanced by estradiol "in situ" production, J. Cell. Physiol. 211 (2007) 448–456.
[60] P. Rizza, I. Barone, D. Zito, F. Giordano, M. Lanzino, F. De Amicis, L. Mauro, D. Sisci, S. Catalano, K.D. Wright, J.A. Gustafsson, S. Ando, Estrogen receptor beta as a novel target of androgen receptor action in breast cancer cell lines, Breast Cancer Res. 16 (2014) R21.
[61] S. Catalano, C. Giordano, P. Rizza, G. Gu, I. Barone, D. Bonofiglio, F. Giordano, R. Malivindi, D. Gaccione, M. Lanzino, F. De Amicis, S. Ando, Evidence that leptin through STAT and CREB signaling enhances cyclin D1 expression and promotes human endometrial cancer proliferation, J. Cell. Physiol. 218 (2009) 490–500.
[62] R. Sirianni, A. Chimento, A. De Luca, I. Casaburi, P. Rizza, A. Onofrio, D. Iacopetta, F. Puoci, S. Ando, M. Maggiolini, V. Pezzi, Oleuropein and hydroxytyrosol inhibit MCF-7 breast cancer cell proliferation interfering with ERK1/2 activation, Mol. Nutr. Food Res. 54 (2010) 833–840.
[63] M.L. Panno, L. Mauro, S. Marsico, D. Bellizzi, P. Rizza, C. Morelli, M. Salerno, F. Giordano, S. Ando, Evidence that the mouse insulin receptor substrate-1 belongs to the gene family on which the promoter is activated by estrogen receptor alpha through its interaction with Sp1, J. Mol. Endocrinol. 36 (2006) 91–105.
[64] D. Sisci, E. Middea, C. Morelli, M. Lanzino, S. Aquila, P. Rizza, S. Catalano, I. Casaburi, M. Maggiolini, S. Ando, 17beta-estradiol enhances alpha(5) integrin subunit gene expression through ERalpha-Sp1 interaction and reduces cell motility and invasion of ERalpha-positive breast cancer cells, Breast Cancer Res. Treat. 124 (2010) 63–77.
[65] S. Catalano, L. Mauro, D. Bonofiglio, M. Pellegrino, H. Qi, P. Rizza, D. Vizza, G. Bossi, S. Ando, In vivo and in vitro evidence that PPARgamma ligands are antagonists of leptin signaling in breast cancer, Am. J. Pathol. 179 (2011) 1030–1040.
[66] A. Carocci, A. Catalano, C. Bruno, A. Lovece, M.G. Roselli, M.M. Cavalluzzi, F. De Santis, A. De Palma, M.R. Rusciano, M. Illario, C. Franchini, G. Lentini, N-(Phenoxyalkyl)amides as MT(1) and MT(2) ligands: antioxidant properties and inhibition of Ca(2+)/CaM-dependent kinase II, Bioorg. Med. Chem. 21 (2013) 847–851.
[67] C. Saturnino, M.S. Sinicropi, O.I. Parisi, D. Iacopetta, A. Popolo, S. Marzocco, G. Autore, A. Caruso, A.R. Cappello, P. Longo, F. Puoci, Acetylated hyaluronic acid: enhanced bioavailability and biological studies, Biomed. Res. Int. 2014 (2014) 921549.
[68] E. Sirignano, A. Pisano, A. Caruso, C. Saturnino, M.S. Sinicropi, R. Lappano, A. Botta, D. Iacopetta, M. Maggiolini, P. Longo, Different 6-Aryl-Fulvenes Exert anti-proliferative effects on Cancer cells, Anticancer Agents Med. Chem. 15 (2015) 468–474.
[69] V. Bartella, P. Rizza, I. Barone, D. Zito, F. Giordano, C. Giordano, S. Catalano, L. Mauro, D. Sisci, M.L. Panno, S.A. Fuqua, S. Ando, Estrogen receptor beta binds Sp1 and recruits a corepressor complex to the estrogen receptor alpha gene promoter, Breast Cancer Res. Treat. 134 (2012) 569–581.
[70] M.S. Sinicropi, A. Caruso, F. Conforti, M. Marrelli, H. El Kashef, J.C. Lancelot, S. Rault, G.A. Statti, F. Menichini, Synthesis, inhibition of NO production and antiproliferative activities of some indole derivatives, J. Enzyme Inhib. Med. Chem. 24 (2009) 1148–1153.
[71] L. Di Donna, D. Iacopetta, A.R. Cappello, G. Gallucci, E. Martello, M. Fiorillo, V. Dolce, G. Sindona, Hypocholesterolaemic activity of 3-hydroxy-3-methylglutaryl flavanones enriched fraction from bergamot fruit (Citrus bergamia): "In vivo" studies, J. Funct. Foods 7 (2014) 558–568.
[72] C. Giordano, S. Catalano, S. Panza, D. Vizza, I. Barone, D. Bonofiglio, L. Gelsomino, P. Rizza, S.A. Fuqua, S. Ando, Farnesoid X receptor inhibits tamoxifen-resistant MCF-7 breast cancer cell growth through downregulation of HER2 expression, Oncogene 30 (2011) 4129–4140.
[73] S. Catalano, C. Giordano, S. Panza, F. Chemi, D. Bonofiglio, M. Lanzino, P. Rizza, F. Romeo, S.A.W. Fuqua, M. Maggiolini, S. Ando, I. Barone, Tamoxifen through GPER upregulates aromatase expression: a novel mechanism sustaining tamoxifen-resistant breast cancer cell growth, Breast Cancer Res. Treat. 146 (2014) 273–285.